


# LASER BEAM PROPAGATION IN NON-KOLMOGOROV ATMOSPHERIC TURBULENCE

THESIS

Bruce Edward Stribling
Captain, USAF

AFIT/GEO/ENG/94D-04





DEPARTMENT OF THE AIR FORCE
AIR UNIVERSITY
AIR FORCE INSTITUTE OF TECHNOLOGY

Wright-Patterson Air Force Base, Ohio

AFIT/GEO/ENG/94D-04

# LASER BEAM PROPAGATION IN NON-KOLMOGOROV ATMOSPHERIC TURBULENCE

THESIS

Bruce Edward Stribling
Captain, USAF

AFIT/GEO/ENG/94D-04

The views expressed in this thesis are those of the author and do not reflect the official policy or position of the Department of Defense or the U. S. Government.

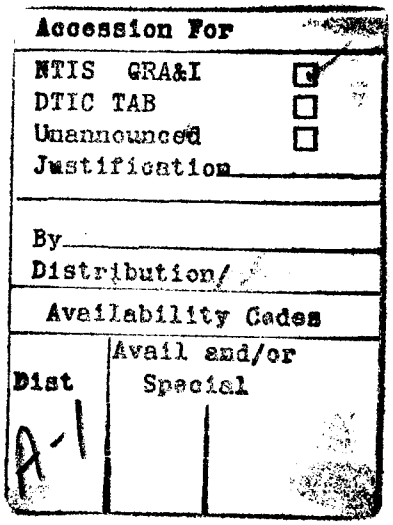

AFIT/GEO/ENG/94D-04

# LASER BEAM PROPAGATION IN NON-KOLMOGOROV ATMOSPHERIC TURBULENCE

THESIS

Presented to the Faculty of the School of Engineering
of the Air Force Institute of Technology
Air University
In Partial Fulfillment of the
Requirements for the Degree of
Master of Science

Bruce Edward Stribling, B.S.E.E.
Captain, USAF

13 Dec, 1994

*Acknowledgements*

First and foremost I would like to thank God, the master creator, for the gifts of forgiveness and everlasting life, and for the wonderfully complex world he has given us to study. May we all use his gifts wisely, to help our fellow man and to ensure the peace.

I would like to thank all the instructors who prepared me to take on such a difficult topic. Maj Micheal Roggemann, Dr. Ted Luke, "Capt Amerika" Dr. Steve Rodgers, you all took the time to help when I needed it. The effort you make in teaching will benefit the Air Force for years to come.

Thank you, Dr. Constantine Houpis for the last minute phone call.

Thank you, Dr. Byron Welsh for your expert guidance and your boundless patience. I'm really sorry for all the meetings I made you late for. No one could ask for better mentor. I only hope we will be able to continue to work together throughout the years.

Thank you, Samantha and Logan for reminding me every night, what's really important in life and not to take myself too seriously.

Last but not least, thank you Debbie, for sacrificing your education so I could continue my own. Thanks for running our family for last 3 years, for cleaning the house, doing the shopping, cooking the meals, ironing my uniforms, remembering where I put my keys and hat, getting the children's birthday presents, reminding me to take out the garbage, and getting us to church on time. You are my soul mate and my best friend. I will love you always. In the true Stribling fashion, it looks like we'll get to Hawaii only 6 months *after* our 10th anniversary. Hopefully the COLA will keep us from being a dollar short. Mahalo and Aloha!

Bruce Edward Stribling

# *Preface*

And God said,

$$\begin{aligned} \nabla \cdot H &= 0 \\ \nabla \times E &= jkH \\ \nabla \times H &= -jkn^2E \\ \nabla \cdot (n^2E) &= 0 \end{aligned}$$

and there was light.

Bruce Edward Stribling

*Table of Contents*

## *List of Figures*

*Abstract*

Several observations of atmospheric turbulence statistics have been reported which do not obey Kolmogorov's power spectral density model. These observations have prompted the study of optical propagation through turbulence described by non-classical power spectra. This thesis presents an analysis of optical propagation through turbulence which causes index of refraction fluctuations to have spatial power spectra that obey arbitrary power laws. The spherical and plane wave structure functions are derived using Mellin transform techniques and are applied to the field mutual coherence function (MCF) using the extended Huygens-Fresnel principle. The MCF is used to compute the Strehl ratio of a focused, constant amplitude beam propagating in non-Kolmogorov turbulence as the power law for the spectrum of the index of refraction fluctuations is varied from -3 to -4. The relative contributions of the log amplitude and phase structure functions to the wave structure function are computed. If inner and outer scale effects are neglected, no turbulence exists when the power law equals -3. At power laws close to -3, the magnitude of the log amplitude and phase perturbations are determined by the system Fresnel ratio. At power laws approaching -4, phase effects dominate in the form of random tilts.

# LASER BEAM PROPAGATION IN NON-KOLMOGOROV ATMOSPHERIC TURBULENCE

## *I. Introduction*

### *1.1 Background*

It is well known that atmospheric turbulence limits the performance of imaging and laser systems. Temperature variations associated with turbulent eddies cause random variations in the index of refraction. This random variation in the index of refraction distorts an optical wave as it propagates through the turbulent atmosphere. The distortions in the optical wave caused by the random index of refraction lead to significant blurring in imaging systems and increased scintillation (twinkling) and wander in a laser beam.

To date, the performance of imaging and laser systems has been estimated assuming the Kolmogorov model for atmospheric turbulence. The Kolmogorov model is a statistical model for the variations of the index of refraction in the atmosphere. The model is defined by a 3-dimensional power spectral density. While the Kolmogorov model has shown good agreement with experiment in the past, recent evidence has shown significant deviations from the Kolmogorov model in certain portions of the atmosphere [1, 4, 6, 7]. The power spectrum of turbulence in portions of the troposphere and stratosphere may exhibit non-Kolmogorov statistics [6, 28]. The propagation of light through turbulence which does not obey Kolmogorov statistics is not well understood.

*1.1.1 Air Force interests in non-Kolmogorov turbulence.* Understanding the propagation of light through non-Kolmogorov turbulence is important to two distinct USAF missions:

1. Theater ballistic missile defense.

   Phillips Laboratory has proposed developing a prototype airborne laser (ABL) system capable of destroying a SCUD-type missile at very long ranges. The system is intended to operate in the troposphere and stratosphere, and requires laser energy to be transmitted to the target over long, horizontal paths. This is precisely where non-Kolmogorov turbulence has been observed [28]. Understanding the effects of non-Kolmogorov turbulence on laser beam propagation may play a key role in determining the operational limits of the ABL concept.

2. Ground-based imaging of space satellites.

   Air Force Space Command has a mission to gather intelligence on foreign satellites in orbit. The mission is accomplished via the use of ground based telescopes. Unfortunately, turbulence limits the resolution that a telescope can achieve. Some turbulence effects can be overcome through the use of adaptive optics. The performance of adaptive optical systems can be further improved by using prior knowledge of turbulence statistics (e.g., Kolmogorov statistics). If the turbulence is modeled as Kolmogorov and is actually non-Kolmogorov through a portion of the atmosphere, the performance of these adaptive optical systems will be degraded.

The research presented in this thesis is primarily devoted to addressing the problems stated above, but has potential application in the areas of laser radar systems and other remote sensing applications, airborne and earth-to-space laser communications systems, and satellite power beaming systems.

*1.1.2 The nature of refractive turbulence and its power spectrum.* Refractive turbulence is generated by the differential heating of the Earth's atmosphere,

winds, and large scale weather phenomena. As large pockets (or eddies) of warm air mix with colder air, energy is transferred from the larger eddies to eddies of smaller sizes. These smaller eddies transfer their energy to still smaller eddies. This energy cascade continues until, at some small scale, viscous effects dominate, the flow becomes laminar and energy is dissipated as heat.

In the seminal work on the statistics of atmospheric turbulence, Kolmogorov [15] derived the structure function for the velocity of a turbulent flow,

$$D_v(r) = \langle [v(\mathbf{r_1} + \mathbf{r}) - v(\mathbf{r_1})]^2 \rangle = C_v^2 r^{2/3} \quad l_o < r < L_o, \tag{1.1}$$

where the angle brackets denote the statistical expectation operator, $v(\mathbf{r_1})$ is the velocity vector at point $\mathbf{r_1}$, $C_v^2$ is the velocity structure constant, the scalar $r$ is the magnitude of the vector $\mathbf{r}$, and $l_o$ and $L_o$ are the inner and outer scales, respectively. The domain of $r$ between $l_o$ and $L_o$ is known as the inertial subrange (See Fig. 1.1). Tatarski [25] used the concept of a conservative passive additive to relate the velocity structure function to the structure function for potential temperature and then, using the Gladstone-Dale relation [5, 21], derived the structure function for the variations in the index of refraction,

$$D_n(r) = \langle [n(\mathbf{r_1} + \mathbf{r}) - n(\mathbf{r_1})]^2 \rangle = C_n^2 r^{2/3} \quad l_o < r < L_o, \tag{1.2}$$

where $n(\mathbf{r_1})$ is the index of refraction at the point $\mathbf{r_1}$ and $C_n^2$ is the index structure constant. It is shown in Chapter 2 that Eq. (1.2) implies the random variations in the index of refraction obey a three dimensional power spectrum given by

$$\Phi_n(\kappa, z) = 0.033 C_n^2(z) \kappa^{-11/3} \quad 2\pi/L_o < \kappa < 2\pi/l_o, \tag{1.3}$$

where $\Phi_n(\kappa, z)$ is the power spectral density as a function of position along the optical path $z$, $\kappa$ is the spatial wavenumber and $C_n^2(z)$ is the index structure constant which

is allowed to vary smoothly along the optical path. $C_n^2(z)$ describes the strength of the turbulence and has units of $\mathrm{m}^{-2/3}$. Equation (1.3) is known as the Kolmogorov power spectrum. The Kolmogorov spectrum agrees well with experiment for vertical propagation paths [21].

The key assumptions in Kolmogorov's and Tatarski's derivations are those of homogeneity and isotropy. For our purposes, "homogeneous" turbulence means the turbulence's power spectrum does not depend on location in the atmosphere. "Isotropic" turbulence means the turbulence's power spectrum does not depend on the direction in which the optical wave is travelling. The Kolmogorov power spectrum is valid in the inertial subrange (see Fig. 1.1), but clearly breaks down for physical reasons at the inner and outer scales. At the inner scale (smallest eddy sizes) the turbulent flow becomes laminar and the kinetic energy of the flow is dissipated as heat. At the outer scale (largest eddy sizes) the spectrum should be limited by the finite size of the atmosphere, thus the assumptions of homogeneity and isotropy are violated. Fortunately, it has been shown that many calculations of interest in propagation theory are insensitive to the exact nature of the power spectrum at the inner and outer scales.

### *1.2 The Existence of Non-Kolmogorov Turbulence*

Von Karman [27], upon examination of Kolmogorov's assumptions, proposed an alternative power spectrum which addresses the problems at the inner and outer scales, but retains the $11/3$ power law in the inertial subrange. Von Karman proposed the following power spectrum,

$$\Phi_n(\kappa, z) = 0.033 C_n^2(z)(\kappa^2 + \kappa_o^2)^{-11/6} \exp\left[-\frac{\kappa^2}{\kappa_m^2}\right] \quad \kappa_o < \kappa < \kappa_m, \tag{1.4}$$

where $\kappa_o = 2\pi/L_o$ and $\kappa_m = 2\pi/l_o$. In many optical calculations involving turbulence, the von Karman spectrum is used for mathematical convenience because it

does not diverge to infinity at zero wavenumber (infinite eddy size). Equation (1.4) also falls off rapidly at the inner scale. The attribute of finite energy coupled with a rapid decrease in energy for increasing wavenumber allows many of the integrals involved in turbulence theory to be evaluated numerically. Figure 1.1 shows the differences between the Kolmogorov and von Karman power spectra.

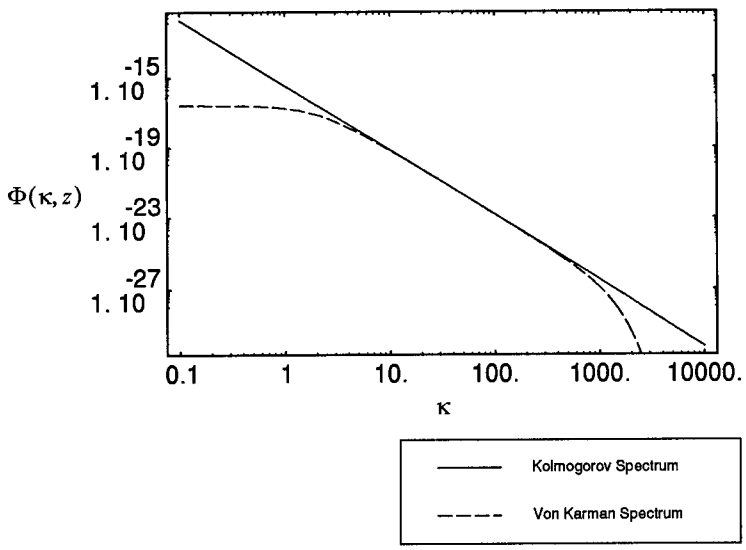


Figure 1.1 Kolmogorov and von Karman power spectra for $C_n^2 = 10^{-14}\mathrm{m}^{-2/3}$. The plot is in terms of spatial wavenumber or $2\pi$/eddy size, thus the inner scale (smallest eddies) are to the right and the outer scale (largest eddies) are to the left. The inertial subrange is the constant slope portion of the von Karman spectrum.

Other authors have proposed extensions of Kolmogorov's work. Greenwood [14] and Hill [13] have found a slight peak before the exponential decay of the inner scale. Gurvich [11] has proposed a local axisymmetric model in place of the isotropic model to account for the existence of buoyancy forces due to temperature differentials between the turbulent eddies.

In addition to these theoretical works, several experimental observations have exhibited peculiar power spectra. Buser [4] has made measurements of turbulence power spectra in the Earth's boundary layer by using a 3-beam Mach-Zender optical interferometer. By interfering several laser beams propagating at different paths through the turbulence and analyzing the interferograms, Buser found that the Kolmogorov theory did not support his measurements. The statistics still obeyed a power law but the observed exponent was significantly lower than 11/3. Buser identified 2 possible explanations for this:

1. At ground level where these measurements were conducted, the conditions for vertical homogeneity and isotropy are most probably violated, especially at larger scale sizes.
2. The buoyancy forces mentioned earlier may be large enough to effect the results of the experiment.

Dayton, et. al. [6], have measured non-Kolmogorov phase structure functions with a Shack-Hartmann wavefront sensor. These measurements imply the existence of non-Kolmogorov turbulence power spectra.

Dalaudier [7] has found direct evidence of temperature sheets in the upper atmosphere. These sheets are areas of strong laminar flow having significant temperature differentials with the surrounding air, thus the conditions of isotropy and homogeneity are not necessarily valid in the upper atmosphere.

Additionally, the existence of non-Kolmogorov turbulence is supported by Wissler's [28] preliminary analysis of the ARGUS anemometer data. The ARGUS anemometer is a high frequency (12kHz) temperature probe mounted near the stagnation point on the nose of a modified RC-135 aircraft. ARGUS has been tasked by Phillips Laboratory to measure refractive turbulence spectra at high altitudes for the Airborne Laser Program (ABL). The index of refraction at high altitude can be estimated by measuring temperature and pressure as a function of the flight path

and relating the measured temperature and pressure to refractive index through the Gladstone-Dale relationship. Many observations of non-Kolmogorov turbulence are believed to exist in the ARGUS data. However, due to the difficulties associated with the frequency response calibration of the anemometer probes, the ARGUS data is inconclusive at this time.

Because of the increasing number of experimental observations of non-Kolmogorov turbulence, it has become necessary to develop a theory which provides a basis for estimating the performance of optical systems in non-Kolmogorov turbulence. For purposes of this thesis, non-Kolmogorov turbulence is defined as turbulence whose three dimensional power spectrum obeys an arbitrary power law,

$$\Phi_n(\kappa, \alpha, z) = a(\alpha)\beta(z)\kappa^{-\alpha}, \tag{1.5}$$

where $\Phi_n(\kappa, \alpha, z)$ is the power spectral density as a function of position along the optical path $z$, $\kappa$ is the spatial wavenumber, $\alpha$ is the power law, $\beta(z)$ is the index structure constant along the path of propagation and has units of $\mathrm{m}^{3-\alpha}$, and $a(\alpha)$ is a function which maintains consistency between the index structure function and its power spectrum (See Eq. 2.49).

## *1.3 Methods for Analyzing the Effects of Turbulence on Laser Beam Propagation*

In order to determine a suitable method to analyze the effects of atmospheric turbulence, one must establish criteria for suitability. For purposes of this research, I use the following criteria:

1. The chosen method must accommodate solutions for an arbitrary wave, not just a plane or spherical wave.
2. The chosen method must accommodate solutions for a turbulence power spectrum which obeys an arbitrary power law.

3. The chosen method must provide good physical insight to the problem. That is, the solution method must separate the geometry of the problem, the statistics of the atmosphere, and the characteristics of the optical wave to be propagated.

Lee and Harp [16], solved the plane wave and spherical wave cases by breaking up the turbulent atmosphere into a sum of thin slabs perpendicular to the propagation path. Each thin slab has its two dimensional refractivity field decomposed into its Fourier components. The effect of each Fourier component of the turbulence acts as a phase diffraction grating on the plane wave. Once these effects have been computed, the authors sum the contributions from each Fourier component in each slab statistically over the path. This approach yields a solution of three multiplicative terms:

1. A term containing the power spectrum of the turbulence.
2. A term relating the fluctuations of a wave at a point in the receiver plane with respect to another point in the receiver.
3. A term which relates the relative efficiency of a turbulent eddy of a certain size, at a certain point in the path, in producing perturbations in the receiver plane. This term is known as a "filter" function.

This method yields more physical insight to the problem, but is still limited to the plane and spherical wave cases.

Lutomirski, Yura, and Buser [17, 18, 30], derived a method for propagating arbitrary fields through turbulence, using the definition of the mutual coherence function (MCF) and the extended Huygens-Fresnel principle. The mutual coherence function of a random wave is the ensemble average of the complex amplitude of the electric field at one point multiplied by the complex amplitude of the field at another point. Mathematically the MCF is given by,

$$MCF(x_1, y_1, x_2, y_2) = \langle U(x_1, y_1) U^*(x_2, y_2) \rangle, \tag{1.6}$$

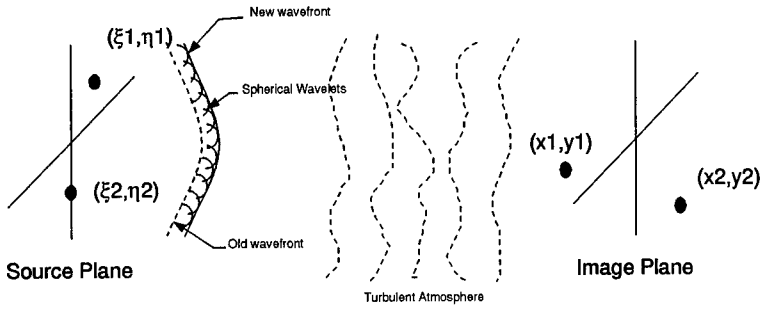


Figure 1.2 A wave propagating from the $\xi, \eta$ plane to the $x, y$ plane, using the extended Huygens-Fresnel principle. The wavefront is the summation of the envelopes of spherical wavelets whose centers where located on an earlier wavefront.

where $U(x_1, y_1)$ and $U(x_2, y_2)$ are the complex amplitudes of the field at the points $(x_1, y_1)$ and $(x_2, y_2)$ and the angle brackets denote the ensemble average. The Huygens-Fresnel principle states (see Fig. 1.2):

> Each point on an optical wave can be regarded as the center of a secondary disturbance which gives rise to spherical wavelets and the position of the wavefront at any later time is the envelope of all such wavelets.

Thus, if one knows how turbulence effects a spherical wave, one can determine the effects of turbulence on an arbitrary wave. The MCF approach provides a solution to the general problem and provides a clear separation between the geometry of the problem, the statistics of the atmosphere, and the wave to be propagated.

Beland [1], in an unpublished work, has used the methods and results of Tatarski [25] and Sasiela [23] to analyze the incoherent imaging case where the turbulence spectrum is non-Kolmogorov. In this work, Beland derives the general expression for the wave structure function for atmospheric turbulence which obeys an arbitrary power law.

By combining Beland's structure function calculation [1] with the methodology of Lutomirski and Buser [17], a method is developed for propagating an arbitrary wave in atmospheric turbulence which obeys an arbitrary power law.

## *1.4 Organization*

In Chapter 2, the mathematical background required for this thesis is introduced. Mellin transform techniques are briefly reviewed. Next, the relationship between the index power spectrum of turbulence and the index structure function is examined. Next, the spherical wave structure function for non-Kolmogorov turbulence is derived and a generalized expression for Fried's coherence diameter $r_o$ is found. Finally, an expression for the variance of the log amplitude fluctuations of an optical wave is defined and the limitations of weak fluctuation theory are examined for various power laws.

Chapter 3 describes the extended Huygens-Fresnel principle for propagation of light in a vacuum and in a random medium. The mutual coherence function of an arbitrary wave in a random medium is derived. The MCF is then used to calculate the on-axis intensities of an arbitrary wave in vacuum and in non-Kolmogorov turbulence.

In Chapter 4, an expression for the Strehl ratio of a focused, constant amplitude wave is derived. The asymptotic behavior of Fried's resolution metric $\mathcal{R}/\mathcal{R}_{\max}$ is examined for various power laws. Additionally, several comparisons of Strehl ratio as a function of the power law are made under various constraints.

In Chapter 5, the relative contributions of the log amplitude and phase structure functions to the wave structure function are addressed.

Chapter 6 discusses the major findings of this research and recommendations for future research.

## *II. Mellin Transforms and the Wave Structure Function*

In order to understand the mathematical development of the non-Kolmogorov propagation theory, one must be familiar with Mellin transform techniques. The Mellin transform is a mathematical tool which allows many complicated real and complex integrals to be evaluated in a straightforward and efficient manner. The first section of this chapter is dedicated to a short review of Mellin transforms. After the section on Mellin transforms, the relationship between the index power spectrum $\Phi_n(\kappa, \alpha, z)$ and the index structure function $D_n(r)$ is derived. This relationship allows one to understand why the power law $\alpha$ of the index power spectrum can only take on certain values. In Section 2.3, the optical wave structure function $D_w(\rho)$ is calculated from the spherical wave correlation function which can be derived from the method of small perturbations. The wave structure function $D_w(\rho)$ will be used extensively in Chapters 3 and 4 to calculate the mutual coherence function (MCF) and Strehl ratio of a laser beam. Since many of the results contained in this research are normalized to atmospheric and path conditions, a generalized version of Fried's coherence diameter $r_o$ is derived. Finally, the limitations of the non-Kolmogorov theory, imposed by the method of small perturbations [2, 5, 25] are examined. The limitations are examined by constraining the variance of the log amplitude fluctuations of the optical field to the regime in which the method of small perturbations is known to agree with experiment.

### *2.1 Introduction to Mellin Transforms*

In many problems in propagation theory we are concerned with integrals of the form

$$h(\alpha) = \int_0^\infty \mathrm{d}\kappa\, \kappa\, \Phi_n(\kappa, \alpha, z) f_1(a_1\kappa^{b_1}) f_2(a_2\kappa^{b_2}) \dots f_n(a_n\kappa^{b_n}), \tag{2.1}$$

where $\Phi_n(\kappa, \alpha, z)$ is the 3-dimensional power spectrum of the turbulence and $f_n(a_n\kappa^{b_n})$ are functions of the integration variable. Because the Mellin transform defined in Eq. (2.2) has a form similar to the integral above (Eq. (2.1)), the Mellin transform is a very useful tool for evaluating integrals associated with propagation of light through turbulence. In this section, the Mellin transform is defined and some of its properties are proven. Euler's gamma function is discussed and some elementary Mellin transforms are evaluated as examples. For more detailed discussions on Mellin transforms, one should refer to the works of Sasiela [22, 23, 24] and Marichev [19].

The Mellin transform and its inverse are defined as

$$H(s) \equiv \mathcal{M}[h(x)] \equiv \int_0^\infty \mathrm{d}x\, x^{s-1} h(x) \tag{2.2}$$

and

$$h(x) \equiv \mathcal{M}^{-1}[H(s)] \equiv \frac{1}{2\pi j} \int_c \mathrm{d}s\, x^s H(s), \tag{2.3}$$

where the path of integration for the inverse transform is a straight line from $-j\infty$ to $j\infty$. The contour $c$ crosses the real axis at a value of $s$ for which the forward transform converges. This strip of the complex plane for which the contour $c$ crosses the real axis is the domain of the transform $\mathcal{D}$.

*2.1.1 Mellin transform properties.* The Mellin transform possesses several properties which can be used to extend a table of Mellin transforms. In this section, the following Mellin transform properties are proven,

$$\mathcal{M}[h(ax)] \rightarrow a^{-s} H(s), \quad a > 0 \tag{2.4}$$

$$\mathcal{M}[x^a h(x)] \rightarrow H(s + a) \tag{2.5}$$

$$\mathcal{M}[h(x^p)] \rightarrow \frac{H(s/p)}{|p|}, \quad p \neq 0. \tag{2.6}$$

**Theorem II.1** *Let $h(x)$ be a Mellin transformable function on domain $\mathcal{D}$, then*

$$\mathcal{M}[h(ax)] \rightarrow a^{-s}H(s) \quad a > 0. \tag{2.7}$$

*Proof:*

$$\mathcal{M}[h(ax)] = \int_0^\infty \mathrm{d}x\, x^{s-1}h(ax) \tag{2.8}$$

*Let*

$$r = ax \quad \mathrm{d}r = a\mathrm{d}x$$
$$x = r/a \quad \mathrm{d}x = \mathrm{d}r/a$$

*then,*

$$\mathcal{M}[h(ax)] = \int_0^\infty \frac{\mathrm{d}r}{a}\left(\frac{r}{a}\right)^{s-1} h(r). \tag{2.9}$$

*Thus,*

$$\mathcal{M}[h(ax)] = a^{-s}\int_0^\infty \mathrm{d}r\, r^{s-1}h(r) \tag{2.10}$$

*and*

$$\mathcal{M}[h(ax)] \rightarrow a^{-s}H(s) \quad a > 0. \tag{2.11}$$

**Theorem II.2** *Let $h(x)$ be a Mellin transformable function on domain $\mathcal{D}$, then*

$$\mathcal{M}[x^a h(x)] \rightarrow H(s+a). \tag{2.12}$$

*Proof:*

$$\mathcal{M}[x^a h(x)] = \int_0^\infty \mathrm{d}x\, x^{s-1}x^a h(x) \tag{2.13}$$

*Let $r = s + a$, then*

$$\mathcal{M}[x^a h(x)] = \int_0^\infty \mathrm{d}x\, x^{r-1}h(x) = H(r), \tag{2.14}$$

*thus,*

$$\mathcal{M}[x^a h(x)] \rightarrow H(s+a). \tag{2.15}$$

**Theorem II.3** *Let $h(x)$ be a Mellin transformable function on domain $\mathcal{D}$, then*

$$\mathcal{M}[h(x^p)] \rightarrow \frac{H(s/p)}{|p|}, \quad p \neq 0. \tag{2.16}$$

*Proof:*

$$\mathcal{M}[h(x^p)] = \int_0^\infty \mathrm{d}x\, x^{s-1} h(x^p) \tag{2.17}$$

*Let*

$$r = x^p \quad \mathrm{d}r = p x^{p-1} \mathrm{d}x$$
$$x = r^{1/p} \quad \mathrm{d}x = \frac{\mathrm{d}r}{p x^{p-1}}$$

*then,*

$$\mathcal{M}[h(x^p)] = \int_0^\infty \frac{\mathrm{d}r}{p(r^{1/p})^{p-1}} r^{\frac{s-1}{p}} h(r). \tag{2.18}$$

*Thus,*

$$\mathcal{M}[h(x^p)] = \frac{1}{p} \int_0^\infty \mathrm{d}r\, r^{\frac{s}{p}-1} h(r) \tag{2.19}$$

*and*

$$\mathcal{M}[h(x^p)] \rightarrow \frac{H(s/p)}{|p|}, \quad p \neq 0. \tag{2.20}$$

*2.1.2 Gamma functions and Mellin transform examples.* Mellin transforms can typically be expressed as ratios of Euler's gamma functions. The gamma function is defined as

$$\Gamma(s) = \int_0^\infty \mathrm{d}x \exp(-x) x^{s-1} = \sum_{n=0}^\infty \frac{(-1)^n}{n!} \frac{1}{s+n} + \int_1^\infty \mathrm{d}x \exp(-x) x^{s-1}. \tag{2.21}$$

The last integral is analytic on the entire complex plane. The gamma function possesses simple poles at the negative integers with residues $(-1)^n/n!$. To express ratios of gamma functions the notation of Sasiela [23] is used,

$$\Gamma\left[\begin{array}{cccc}\alpha_1 & \alpha_2 & \dots & \alpha_m \\ \beta_1 & \beta_2 & \dots & \beta_n\end{array}\right] = \frac{\Gamma[\alpha_1]\Gamma[\alpha_2]\dots\Gamma[\alpha_m]}{\Gamma[\beta_1]\Gamma[\beta_2]\dots\Gamma[\beta_n]}. \tag{2.22}$$

Most of the integrals in this thesis can be evaluated by a simple change of variables and a table lookup, just as in Fourier transform theory. Tables can be found in Sasiela [22, 23, 24] and Marichev [19]. The example below is from a problem discussed in the following section.

**Example II.1** *In the Section 2.2, we wish to find the power spectrum associated with a structure function that obeys an arbitrary power law. Tatarski derived the following relation,*

$$\Phi_n(\kappa) = \frac{1}{4\pi^2\kappa^2}\int_0^\infty \frac{\sin(\kappa r)}{\kappa r}\frac{\mathrm{d}}{\mathrm{d}r}\left[r^2\frac{\mathrm{d}}{\mathrm{d}r}D_n(r)\right]\mathrm{d}r, \tag{2.23}$$

*where $\Phi_n(\kappa)$ is the isotropic 3-dimensional turbulence power spectrum and $D_n(r)$ is the index structure function. Substituting the index structure function $D_n(r) = \beta(z)r^\gamma$ (See Eq. (2.52)) into Eq. (2.23) and evaluating the derivatives yields*

$$\Phi_n(\kappa, z) = \frac{\beta(z)(\gamma^2+\gamma)}{4\pi^2\kappa^2}\int_0^\infty \mathrm{d}r\,\frac{\sin(\kappa r)}{\kappa r}r^\gamma. \tag{2.24}$$

*Making a change of variables*

$$x = \kappa r \quad \mathrm{d}x = \kappa \mathrm{d}r$$
$$r = x/\kappa \quad \mathrm{d}r = \mathrm{d}x/\kappa,$$

*Eq. (2.24) becomes*

$$\Phi_n(\kappa, z) = \frac{\beta(z)(\gamma^2+\gamma)}{4\pi^2\kappa^{3+\gamma}} \int_0^\infty \mathrm{d}x\, x^{\gamma-1} \sin(x). \tag{2.25}$$

*Equation (2.25) is the Mellin transform of* $\sin(x)$. *Using the transform*

$$\mathcal{M}[\sin(x)] \rightarrow 2^{s-1}\sqrt{\pi}\Gamma\left[\begin{array}{c} 1/2+s/2 \\ 1-s/2 \end{array}\right] \quad |\Re(s)| < 1, \tag{2.26}$$

*Eq. (2.25) becomes*

$$\Phi_n(\kappa, z) = 2^{\gamma-3}\beta(z)(\gamma^2+\gamma)\pi^{-3/2}\Gamma\left[\begin{array}{c} \frac{1+\gamma}{2} \\ \frac{2-\gamma}{2} \end{array}\right] \kappa^{-(3+\gamma)} \quad |\gamma| < 1. \tag{2.27}$$

*By defining* $\alpha = \gamma + 3$, *Eq. (2.27) becomes,*

$$\Phi_n(\kappa, z) = 2^{\alpha-6}\beta(z)(\alpha^2-5\alpha+6)\pi^{-3/2}\frac{\Gamma\left[\frac{\alpha-2}{2}\right]}{\Gamma\left[\frac{5-\alpha}{2}\right]}\kappa^{-\alpha} \quad 2 < \alpha < 4. \tag{2.28}$$

*Notice the domain in Eq. (2.28) differs from Eq. (2.54) and Eq. (2.57). Equation (2.28) must be analytically continued to the domain* $3 < \alpha < 5$, *to ensure the power spectral density is positive. The analytic continuation is done automatically in the next example.*

In many turbulence problems it is necessary to evaluate the Mellin transform of a function minus the first term of its power series. The resultant transform is the same as the original function but the domain of the transform has moved past one pole. This is demonstrated in the following example.

**Example II.2** *To derive Beland's [1] expression for $a(\alpha)$ in Eq. (1.5) we can use Eq. (2.48) which is derived later in the chapter,*

$$D_n(r,z) = 8\pi \int_0^\infty \mathrm{d}\kappa\, \Phi_n(\kappa,z)\kappa^2 \left[1 - \frac{\sin(\kappa r)}{\kappa r}\right]. \tag{2.29}$$

*Substituting the definitions for the index structure function $D_n(r,z) = \beta(z)r^\gamma$ and turbulence power spectrum $\Phi_n(\kappa,z) = a(\alpha)\beta(z)\kappa^{-\alpha}$ (See Eq. (2.52) and Eq. (2.56)) into Eq. (2.29) yields*

$$r^\gamma = 8\pi a(\alpha) \int_0^\infty \mathrm{d}\kappa\kappa^{2-\alpha} \left[1 - \frac{\sin(\kappa r)}{\kappa r}\right]. \tag{2.30}$$

*Letting $s = 3 - \alpha$ and making the change of variables,*

$$\begin{aligned} x &= \kappa r \quad \mathrm{d}x = r\mathrm{d}\kappa \\ \kappa &= x/r \quad \mathrm{d}\kappa = \mathrm{d}x/r, \end{aligned} \tag{2.31}$$

*Eq. (2.30) becomes*

$$r^\gamma = 8\pi a(\alpha) r^{\alpha-3} \int_0^\infty \mathrm{d}x\, x^{s-1} \left[1 - \frac{\sin(x)}{x}\right]. \tag{2.32}$$

*Multiplying Eq. (2.32) by $-1$ yields*

$$r^\gamma = -8\pi a(\alpha) r^{\alpha-3} \int_0^\infty \mathrm{d}x\, x^{s-1} \left[x^{-1}\sin(x) - 1\right]. \tag{2.33}$$

*Applying the Mellin transforms*

$$\begin{aligned} \mathcal{M}[x^a h(x)] &\rightarrow H(s+a) \\ \mathcal{M}[\sin(x)] &\rightarrow 2^{s-1}\sqrt{\pi}\Gamma\left[\begin{array}{c} 1/2 + s/2 \\ 1 - s/2 \end{array}\right] \quad |\Re(s)| < 1 \end{aligned}$$

$$\mathcal{M}[1] \quad \rightarrow \lim_{\epsilon\rightarrow 0}\left[\frac{1}{s+\epsilon}-\frac{1}{s-\epsilon}\right] \qquad |\Re(s)|<\epsilon \tag{2.34}$$

*yields*

$$r^{\gamma} = -8\pi a(\alpha) r^{\alpha-3} \lim_{\epsilon\rightarrow 0}\left\{2^{s-2}\sqrt{\pi}\Gamma\begin{bmatrix} s/2 \\ (3-s)/2 \end{bmatrix} - \frac{1}{s+\epsilon}+\frac{1}{s-\epsilon}\right\} \qquad |\Re(s)|<\epsilon. \tag{2.35}$$

*In the limit as* $\epsilon \rightarrow 0$ *the poles at* 0 *and* $-\epsilon$ *additively cancel and the domain becomes* $-2<\Re(s)<0$. *Since* $s=3-\alpha$, *Eq. (2.35) becomes*

$$r^{\gamma} = -8\pi a(\alpha) r^{\alpha-3} 2^{1-\alpha}\sqrt{\pi}\Gamma\begin{bmatrix} (3-\alpha)/2 \\ \alpha/2 \end{bmatrix} \quad 3<\alpha<5. \tag{2.36}$$

*Equating the exponents of* $r$ *and solving for* $a(\alpha)$ *yields*

$$a(\alpha) = -(2)^{\alpha-4}\pi^{-3/2}\Gamma\begin{bmatrix} \alpha/2 \\ (3-\alpha)/2 \end{bmatrix} \quad 3<\alpha<5. \tag{2.37}$$

*The moving of a domain past a pole is an example of an analytic continuation of a function.*

## *2.2 The Relationship Between the Index Power Spectrum and the Index Structure Function*

The random variations in the index of refraction can be described by the three dimensional autocorrelation function

$$\Gamma_n(\vec{\mathbf{r_1}},\vec{\mathbf{r_2}}) = \mathcal{E}\left\{n(\vec{\mathbf{r_1}})n(\vec{\mathbf{r_2}})\right\}, \tag{2.38}$$

where $n(\vec{\mathbf{r_1}})$ and $n(\vec{\mathbf{r_2}})$ are the indices of refraction at points $\vec{\mathbf{r_1}}$ and $\vec{\mathbf{r_2}}$ and $\mathcal{E}$ is the expectation operator. By assuming that the index variations are homogeneous (stationary) throughout the atmosphere, the autocorrelation function can be expressed as a function of difference coordinates only,

$$\Gamma_n(\vec{\mathbf{r}}) = \mathcal{E}\left\{n(\vec{\mathbf{r_1}})n(\vec{\mathbf{r_1}} - \vec{\mathbf{r}})\right\}, \tag{2.39}$$

where $\vec{\mathbf{r}} = \vec{\mathbf{r_2}} - \vec{\mathbf{r_1}}$. The Weiner-Khinchine theorem states the autocorrelation and power spectral density of a wide sense stationary random process are Fourier transform pairs, therefore

$$\Phi_n(\vec{\kappa}) = \frac{1}{(2\pi)^3}\iiint \Gamma_n(\vec{\mathbf{r}})e^{j\vec{\kappa}\cdot\vec{\mathbf{r}}}\mathrm{d}^3\vec{\mathbf{r}}. \tag{2.40}$$

Assuming the turbulence is isotropic (i.e., $\Gamma_n(\vec{\mathbf{r}})$ depends only on $r = |\vec{\mathbf{r}}|$), Eq. (2.40) can be written as a single integral [3],

$$\Phi_n(\kappa) = \frac{1}{2\pi^2\kappa}\int_0^\infty r\Gamma_n(r)\sin(\kappa r)\mathrm{d}r \tag{2.41}$$

and the inverse relationship is

$$\Gamma_n(r) = \frac{4\pi}{r}\int_0^\infty \kappa\Phi_n(\kappa)\sin(\kappa r)\mathrm{d}\kappa. \tag{2.42}$$

For isotropic turbulence, Eq. (2.41) and Eq. (2.42) are the fundamental relationship between the autocorrelation of index variations and the index power spectrum. It is through the use of Eq. (2.41) that the index structure function, defined below, is related to the index power spectrum.

An extremely useful method of describing the random variations in the index of refraction is through the use of structure functions. The structure function of the

index of refraction variations is defined as

$$D_n(\vec{\mathbf{r_1}}, \vec{\mathbf{r_2}}) = \mathcal{E}\left\{[n(\vec{\mathbf{r_1}}) - n(\vec{\mathbf{r_2}})]^2\right\}. \tag{2.43}$$

Expanding Eq. (2.43) and applying the linearity of the expectation operator yields

$$D_n(\vec{\mathbf{r_1}}, \vec{\mathbf{r_2}}) = \mathcal{E}\left\{n(\vec{\mathbf{r_1}})^2\right\} - 2\mathcal{E}\left\{n(\vec{\mathbf{r_1}})n(\vec{\mathbf{r_2}})\right\} + \mathcal{E}\left\{n(\vec{\mathbf{r_2}})^2\right\}. \tag{2.44}$$

Since the turbulence is assumed wide sense stationary,

$$\mathcal{E}\left\{n(\vec{\mathbf{r_1}})^2\right\} = \mathcal{E}\left\{n(\vec{\mathbf{r_2}})^2\right\} = \Gamma_n(0). \tag{2.45}$$

Thus, the index structure function for isotropic turbulence can be written

$$D_n(r) = 2[\Gamma_n(0) - \Gamma_n(r)]. \tag{2.46}$$

Substituting Eq. (2.42) into Eq. (2.46) yields

$$D_n(r) = 2\left[\lim_{r\to 0}\left\{\frac{4\pi}{r}\int_0^\infty \kappa\Phi_n(\kappa)\sin(\kappa r)\mathrm{d}\kappa\right\} - \frac{4\pi}{r}\int_0^\infty \kappa\Phi_n(\kappa)\sin(\kappa r)\mathrm{d}\kappa\right], \tag{2.47}$$

where the limit on the first term is required because of the pole at $r = 0$. Evaluating the limit yields

$$D_n(r) = 8\pi\int_0^\infty \Phi_n(\kappa)\kappa^2\left[1 - \frac{\sin(\kappa r)}{\kappa r}\right]\mathrm{d}\kappa. \tag{2.48}$$

Tatarski [26] solved for the inverse of Eq. (2.48) in terms of the derivatives of the structure function,

$$\Phi_n(\kappa) = \frac{1}{4\pi^2\kappa^2}\int_0^\infty \frac{\sin(\kappa r)}{\kappa r}\frac{\mathrm{d}}{\mathrm{d}r}\left[r^2\frac{\mathrm{d}}{\mathrm{d}r}D_n(r)\right]\mathrm{d}r. \tag{2.49}$$

Equation (2.49) can be used to find the power spectrum from a given structure function. For example, Tatarski [25] derived the index structure function in terms

of Kolmogorov's inertial subrange model

$$D_n(r,z) = C_n^2(z) r^{2/3}. \tag{2.50}$$

By substituting Eq. (2.50) into Eq. (2.49) one can show

$$\Phi_n(\kappa,z) = 0.033 C_n^2(z) \kappa^{-11/3}. \tag{2.51}$$

To find the power spectrum associated with an arbitrary structure function,

$$D_n(r,z) = \beta(z) r^{\gamma}, \tag{2.52}$$

one substitutes Eq. (2.52) into Eq. (2.49) and evaluates the integral. In Example II.2 $\gamma$ was shown to be $\gamma = \alpha - 3$, thus,

$$D_n(r,\alpha,z) = \beta(z) r^{\alpha-3}. \tag{2.53}$$

The power spectrum of the turbulence in terms of the arbitrary power law structure function was shown in Example II.1 of the previous section to be,

$$\Phi_n(\kappa,z) = 2^{\alpha-6}\beta(z)(\alpha^2-5\alpha+6)\pi^{-3/2}\frac{\Gamma\left[\frac{\alpha-2}{2}\right]}{\Gamma\left[\frac{5-\alpha}{2}\right]}\kappa^{-\alpha} \quad 3<\alpha<5, \tag{2.54}$$

where $\beta(z)$ is the structure constant similar to $C_n^2(z)$ and has units of $\mathrm{m}^{3-\alpha}$, $\Gamma[x]$ is Euler's gamma function, and the power law $\alpha$ is defined as $\alpha \equiv \gamma + 3$. The function $a(\alpha)$ which maintains consistency between the index structure function and its power spectrum (See Eq. (2.49)) is found by equating Eq. (1.5) and Eq. (2.54) and solving for $a(\alpha)$:

$$a(\alpha) \equiv 2^{\alpha-6}(\alpha^2-5\alpha+6)\pi^{-3/2}\frac{\Gamma\left[\frac{\alpha-2}{2}\right]}{\Gamma\left[\frac{5-\alpha}{2}\right]} \quad 3<\alpha<5. \tag{2.55}$$

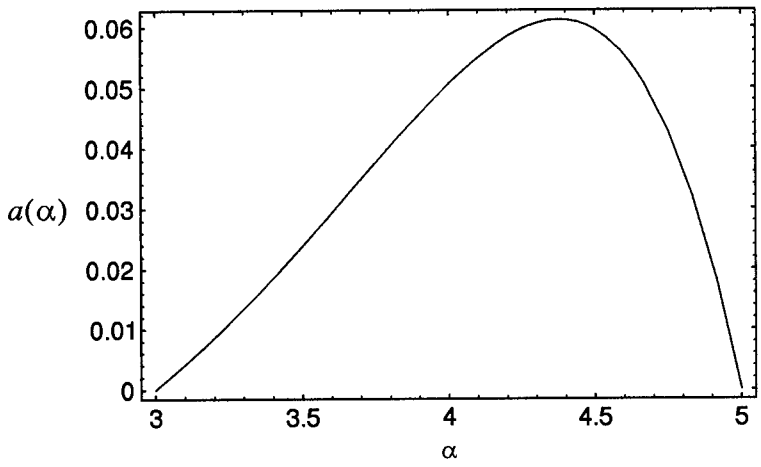


Figure 2.1 The consistency function $a(\alpha)$.

This result is mathematically equivalent to Eq. (2.37) derived in Example II.2 and Eq. (2.57) below. The consistency function $a(\alpha)$ is plotted in Fig. (2.1). Thus, the index power spectrum for an arbitrary power law is

$$\Phi_n(\kappa, \alpha, z) = a(\alpha)\beta(z)\kappa^{-\alpha}. \tag{2.56}$$

Equation (2.56) reduces to the Kolmogorov power spectrum (Eq. (2.51)) if $\alpha = 11/3$. Note that Beland [1] has derived an alternate but equivalent definition for $a(\alpha)$ [1],

$$a(\alpha) \equiv -(2)^{\alpha-4}\pi^{-3/2}\frac{\Gamma\left[\frac{\alpha}{2}\right]}{\Gamma\left[\frac{3-\alpha}{2}\right]} \quad 3 < \alpha < 5. \tag{2.57}$$

[1]This problem was solved as an example in the previous section on Mellin transforms.

Equations (2.52) and (2.54) yield a very important physical interpretation. If the inner and outer scale effects are neglected, the power law $\alpha$ must be greater than 3, because when $\alpha \to 3$, $a(\alpha) \to 0$ and the turbulence power spectrum vanishes. Likewise, the index structure function has no dependence on the separation $r$ (i.e., $D_n(r,z) = \beta(z)r^0$), implying no random turbulence exists. We will see in the next section that the domain of $\alpha$ is further constrained in the wave structure function calculation.

### *2.3 The Wave Structure Function*

In order to estimate the effects of turbulence on optical wave propagation, one must solve the wave equation for a random media,

$$\nabla^2\vec{\mathbf{E}} + k^2n^2\vec{\mathbf{E}} = 0, \tag{2.58}$$

where $n$ is a random field of index variations over the region of propagation. If the turbulence is weak, homogeneous, and isotropic, the method of small perturbations can be used to solve Eq. (2.58) [2, 5, 10, 25]. The method of small perturbations yields the two dimensional spherical wave correlation functions (in a plane transverse to the direction of propagation) for the log amplitude and phase,

$$B_\chi(\rho) = 4\pi^2k^2\int_0^L \mathrm{d}z \int_0^\infty \mathrm{d}\kappa\,\kappa J_0\left(\frac{\kappa\rho z}{L}\right)\sin^2\left[\frac{\kappa^2 z(L-z)}{2kL}\right]\Phi_n(\kappa,z) \tag{2.59}$$

and

$$B_\phi(\rho) = 4\pi^2k^2\int_0^L \mathrm{d}z \int_0^\infty \mathrm{d}\kappa\,\kappa J_0\left(\frac{\kappa\rho z}{L}\right)\cos^2\left[\frac{\kappa^2 z(L-z)}{2kL}\right]\Phi_n(\kappa,z), \tag{2.60}$$

where $J_0$ is a Bessel function of the first kind, order 0, $k$ is the optical wavenumber, $\rho$ is the geometrical separation between points in the plane, and $L$ is the length of the optical path.

In this section, the wave structure function for non-Kolmogorov turbulence $D_w(\rho)$ is derived using Eq. (2.59) and Eq. (2.60). The wave structure function is defined as the sum of the log-amplitude and the phase structure functions,

$$D_w(\rho) = D_\chi(\rho) + D_\phi(\rho). \tag{2.61}$$

The relations

$$D_\chi(r) = 2[B_\chi(0) - B_\chi(r)], \tag{2.62}$$

and

$$D_\phi(r) = 2[B_\phi(0) - B_\phi(r)], \tag{2.63}$$

can be derived in a fashion similar to Eq. (2.43). Using Eqs. (2.62) and (2.63) and substituting Eqs. (2.56), (2.59) and (2.60) into Eq. (2.61) yields

$$D_w(\rho) = 8\pi^2 k^2 a(\alpha) \int_0^L \beta(z) \int_0^\infty \kappa^{1-\alpha} \left[1 - J_0(\frac{\kappa\rho z}{L})\right] \mathrm{d}\kappa \mathrm{d}z, \tag{2.64}$$

where $a(\alpha)$ is the consistency function, $\beta(z)$ is the index structure constant along the optical path, $\kappa$ is the spatial wavenumber of the turbulent eddies, $J_0$ is a Bessel function of the first kind, order 0, and $\rho$ is the geometric distance between two points in the plane transverse to the direction of propagation. Equation (2.64) can be evaluated using Mellin transforms. Sasiela [23] gives the necessary identity,

$$\mathcal{M}[1 - J_0(x)] = -2^{s-1} \frac{\Gamma(\frac{s}{2})}{\Gamma(\frac{2-s}{2})} \quad -2 < \Re(s) < 0, \tag{2.65}$$

where $\Gamma$ is Euler's gamma function. Making the change of variables

$$x = \frac{\kappa\rho z}{L} \quad \mathrm{d}x = \tfrac{\rho z}{L}\mathrm{d}\kappa$$
$$\kappa = \frac{xL}{\rho z} \quad \mathrm{d}\kappa = \tfrac{L}{\rho z}\mathrm{d}x$$

and letting $s = 2 - \alpha$, Eq. (2.64) becomes

$$D_w(\rho) = 8\pi^2 k^2 a(\alpha) \int_0^L \beta(z) \int_0^\infty \frac{L}{\rho z} \left(\frac{xL}{\rho z}\right)^{1-\alpha} [1 - J_0(x)] \mathrm{d}x \mathrm{d}z. \tag{2.66}$$

Rearranging terms yields

$$D_w(\rho) = 8\pi^2 k^2 a(\alpha) L^{2-\alpha} \rho^{\alpha-2} \int_0^L \beta(z) z^{\alpha-2} \mathrm{d}z \int_0^\infty x^{s-1} [1 - J_0(x)] \mathrm{d}x. \tag{2.67}$$

Applying the Mellin transform in Eq. (2.65) and remembering $a(\alpha)$ is defined from $3 < \alpha < 5$,

$$D_w(\rho) = -(2)^{4-\alpha} \pi^2 k^2 a(\alpha) L^{2-\alpha} \rho^{\alpha-2} \Gamma \left[ \begin{matrix} \frac{2-\alpha}{2} \\ \frac{\alpha}{2} \end{matrix} \right] \int_0^L \beta(z) z^{\alpha-2} \mathrm{d}z \quad 3 < \alpha < 4. \tag{2.68}$$

If $\beta(z)$ is constant over the optical path, Eq. (2.68) can be simplified. Evaluating the integral for this case yields

$$D_w(\rho) = -(2)^{4-\alpha} \pi^2 k^2 a(\alpha) L^{2-\alpha} \rho^{\alpha-2} \Gamma \left[ \begin{matrix} \frac{2-\alpha}{2} \\ \frac{\alpha}{2} \end{matrix} \right] \beta \frac{L^{\alpha-1}}{\alpha - 1} \quad 3 < \alpha < 4. \tag{2.69}$$

Rearranging Eq. (2.69) yields,

$$D_w(\rho) = -(2)^{4-\alpha} \pi^2 k^2 a(\alpha) \beta L \frac{\Gamma(\frac{2-\alpha}{2})}{(\alpha - 1)\Gamma(\frac{\alpha}{2})} \rho^{\alpha-2} \quad 3 < \alpha < 4. \tag{2.70}$$

Equation (2.70) is the spherical wave structure function for turbulence characterized by an arbitrary power law $\alpha$. To get the plane wave structure function one excludes the $(\alpha - 1)$ term in the denominator of Eq. (2.70). Equation (2.70) will be used extensively in Chapters 3 and 4 to compute the mutual coherence function and Strehl ratio of a laser beam.

## 2.4 *A Generalized Expression for Fried's Coherence Diameter $r_o$*

Many of the results in this thesis are normalized by atmospheric and path conditions. Fried [8, 9] accomplished the normalization by defining a "coherence diameter", $r_o$, which takes into account the strength of the turbulence and the path length. Fried [8] defines the plane wave structure function as

$$D_w(\rho) = 6.88 \left(\frac{\rho}{r_o}\right)^{5/3} \tag{2.71}$$

where

$$r_o = \left(\frac{6.88}{2.91k^2 \int_0^L C_n^2(z)\mathrm{d}z}\right)^{3/5}. \tag{2.72}$$

The arbitrary constant 6.88 is defined more accurately in [8] as $2(24/5\Gamma(6/5))^{5/6}$. This constant was chosen to force Fried's resolution metric $\mathcal{R}/\mathcal{R}_{\max}$ [8] to have a certain asymptotic behavior. Since Fried's definition of $r_o$ only applies to an 11/3 power law in the Kolmogorov spectrum, a more general expression is presented here.

Our definition for the spherical wave structure function is rewritten from Eq. (2.70)

$$D_w(\rho) = -(2)^{4-\alpha}\pi^2 k^2 a(\alpha) L^{2-\alpha}\rho^{\alpha-2}\Gamma\left[\begin{array}{c}\frac{2-\alpha}{2}\\ \frac{\alpha}{2}\end{array}\right]\int_0^L \beta(z) z^{\alpha-2}\mathrm{d}z \quad 3<\alpha<4. \tag{2.73}$$

We need to find a parameter $\rho_o$, which reduces to $r_o$ when the power law $\alpha \to 11/3$, such that

$$D_w(\rho) = c_1 \left(\frac{\rho}{\rho_o}\right)^{\alpha-2}, \tag{2.74}$$

where

$$c_1 = 2\left(\frac{8}{\alpha-2}\Gamma\left[\frac{2}{\alpha-2}\right]\right)^{\frac{\alpha-2}{2}}. \tag{2.75}$$

The choice of $c_1$ will become more apparent when the asymptotic behavior of Fried's $\mathcal{R}/\mathcal{R}_{max}$ is discussed in Chapter 4. Setting Eq. (2.73) equal to Eq. (2.74) and

solving for $\rho_o$ yields

$$\rho_o = \left\{ \frac{c_1(\alpha-1)\Gamma\left[\frac{\alpha}{2}\right]}{-(2)^{4-\alpha}\pi^2 k^2 a(\alpha) L^{2-\alpha}\Gamma\left[\frac{2-\alpha}{2}\right]\int_0^L \beta(z) z^{\alpha-2} \mathrm{d}z} \right\}^{\frac{1}{\alpha-2}} \quad 3 < \alpha < 4. \quad (2.76)$$

If $\beta(z)$ is constant over the path then Eq. (2.76) reduces to

$$\rho_o = \left\{ \frac{c_1(\alpha-1)\Gamma\left[\frac{\alpha}{2}\right]}{-(2)^{4-\alpha}\pi^2 k^2 a(\alpha)\Gamma\left[\frac{2-\alpha}{2}\right]\beta L} \right\}^{\frac{1}{\alpha-2}} \quad 3 < \alpha < 4. \quad (2.77)$$

Again, for the plane wave expression of $\rho_o$ the $(\alpha - 1)$ term is omitted.

Figure (2.2) is a plot of $\rho_o$ as a function of $\alpha$ for various values of $\beta L$. It is important to note that $\rho_o$ scales with $\lambda^{2/(\alpha-2)}$. In Section 2.2, it was shown that

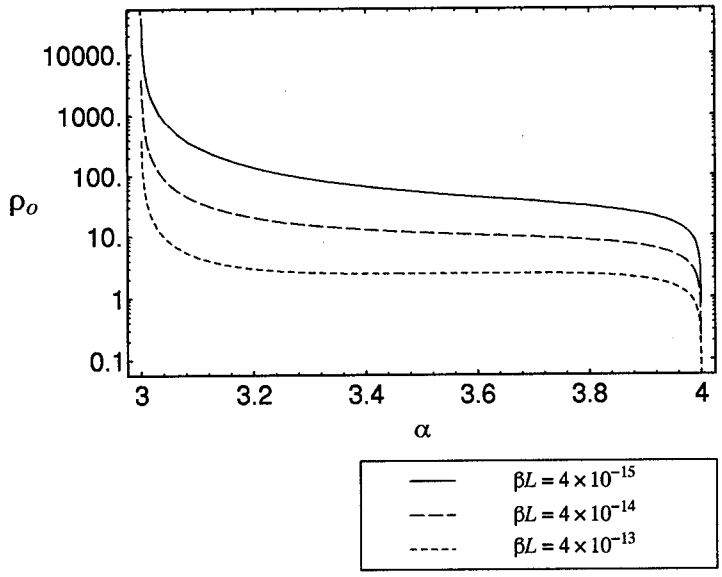


Figure 2.2 The generalized coherence diameter $\rho_o$ as a function of $\alpha$ normalized by $\beta L$. The wavelength is 1.3 microns.

turbulence with power laws $\alpha \leq 3$ can not exist, because the index structure function has no dependence on $r$ when $\alpha = 3$. This is reflected in Fig. (2.2) as well, since $\rho_o \rightarrow \infty$ when $\alpha \rightarrow 3$. When $\alpha \rightarrow 4$ we see $\rho_o \rightarrow 0$, this can be explained by the square law dependence of the wave structure function (Eq. (2.74) when $\alpha = 4$. Heidbreder [12] showed that the phase structure function in the near field limit, which is equivalent to the wave structure function presented here, induces pure random tilt on the wavefront. Since a pure random tilt shifts the beam off axis for each realization of turbulence (short exposure) the average irradiance (long exposure) will be the average of the unabberated beam shifted all over the observation plane. This results in a wide spot with a very low irradiance peak. This is exactly what is happening in Fig. (2.2). The worst turbulence to have in an uncompensated beam projection system is turbulence whose structure function only induces tilt on the wavefront, thereby shifting its short exposure spot continually around the observation plane. This effect will be discussed further in Chapter 4.

## *2.5 The Variance of the Log Amplitude Fluctuations and Limitations of the Theory*

Using the method of small perturbations to solve the wave equation (See Eq. (2.58)) is limited to regimes where the tubulence is weak and the propagation distance is short. For Kolmogorov turbulence the method of small perturbations has been shown to be valid when the log amplitude variance is small (for $\sigma_\chi^2 \leq 0.3 - 0.5$) [5]. When the log amplitude variance is greater than $0.3 - 0.5$ a multiple scattering theory is required. For purposes of this discussion, it is assumed the criterion $\sigma_\chi^2 \leq 0.3 - 0.5$ holds for propagation in an arbitrary power law turbulence spectrum. To prove the relation $\sigma_\chi^2 \leq 0.3 - 0.5$ holds for an arbitrary power law turbulence spectrum requires comparison with a multiple scattering theory which is beyond the scope of this thesis.

One can examine the variance of the log amplitude perturbations in order to understand the bounds the method of small perturbations places on turbulence

strength and range as the power law of the turbulence spectrum varies. Here the bounds are found by constraining the log amplitude variance to $0.1 - 0.5$ and solving for the system and atmospheric parameters of interest. From the plane wave correlation function [2],

$$\sigma_\chi^2 = B_\chi(0) = 4\pi^2 k^2 \int_0^L \mathrm{d}z \int_0^\infty \mathrm{d}\kappa\, \kappa \sin^2\left[\frac{\kappa^2(L-z)}{2k}\right] \Phi_n(\kappa, \alpha, z). \tag{2.78}$$

Substituting the turbulence spectrum given by Eq. (2.56) into Eq. (2.78) yields

$$\sigma_\chi^2 = 4\pi^2 k^2 \int_0^L \mathrm{d}z\, \beta(z) \int_0^\infty \mathrm{d}\kappa\, \kappa^{1-\alpha} \sin^2\left[\frac{\kappa^2(L-z)}{2k}\right]. \tag{2.79}$$

Letting $s = 2 - \alpha$ and $w = \frac{L-z}{2k}$ gives

$$\sigma_\chi^2 = 4\pi^2 k^2 a(\alpha) \int_0^L \mathrm{d}z\, \beta(z) \int_0^\infty \mathrm{d}\kappa\, \kappa^{s-1} \sin^2\left[w\kappa^2\right]. \tag{2.80}$$

Making the change of variable $x = \sqrt{w}\kappa$ and $\mathrm{d}x = \sqrt{w}\mathrm{d}\kappa$ yields

$$\sigma_\chi^2 = 4\pi^2 k^2 a(\alpha) \int_0^L \mathrm{d}z\, \beta(z) \int_0^\infty \frac{\mathrm{d}x}{\sqrt{w}} \left(\frac{x}{\sqrt{w}}\right)^{s-1} \sin^2\left[x^2\right]. \tag{2.81}$$

Simplifying Eq. (2.81) gives

$$\sigma_\chi^2 = 4\pi^2 k^2 a(\alpha) \int_0^L \mathrm{d}z\, w^{-s/2} \beta(z) \int_0^\infty \mathrm{d}x\, (x)^{s-1} \sin^2\left[x^2\right]. \tag{2.82}$$

Equation (2.82) is the Mellin transform of $\sin^2(x^2)$. The applicable transform pair is

$$M[\sin^2(x^2)] \rightarrow -\frac{\sqrt{\pi}}{8}\Gamma\begin{bmatrix} s/4 \\ 1/2 - s/4 \end{bmatrix} \quad -4 < \Re(s) < 0, \tag{2.83}$$

thus,

$$\sigma_\chi^2 = -4\pi^2 k^2 a(\alpha) \int_0^L \mathrm{d}z\, w^{-s/2} \beta(z) \frac{\sqrt{\pi}}{8} \Gamma \left[ \begin{matrix} \frac{2-\alpha}{4} \\ \frac{\alpha}{4} \end{matrix} \right] \quad 2 < \alpha < 6. \tag{2.84}$$

Substituting for $w$,

$$\sigma_\chi^2 = -\frac{1}{2} \pi^{5/2} k^2 a(\alpha) \int_0^L \mathrm{d}z \left( \frac{L-z}{2k} \right)^{\frac{\alpha-2}{2}} \beta(z) \Gamma \left[ \begin{matrix} \frac{2-\alpha}{4} \\ \frac{\alpha}{4} \end{matrix} \right] \quad 2 < \alpha < 6. \tag{2.85}$$

Simplifying Eq. (2.85) and remembering $a(\alpha)$ is defined on $3 < \alpha < 5$ gives

$$\sigma_\chi^2 = -2^{-\alpha/2} \pi^{5/2} k^{\frac{6-\alpha}{2}} a(\alpha) \Gamma \left[ \begin{matrix} \frac{2-\alpha}{4} \\ \frac{\alpha}{4} \end{matrix} \right] \int_0^L \mathrm{d}z \beta(z) \left( L - z \right)^{\frac{\alpha-2}{2}} \quad 3 < \alpha < 5. \tag{2.86}$$

If $\beta(z)$ is constant along the path, then we have

$$\sigma_\chi^2 = -\frac{2^{\frac{2-\alpha}{2}} \pi^{5/2} k^{\frac{6-\alpha}{2}} a(\alpha)}{\alpha} \Gamma \left[ \begin{matrix} \frac{2-\alpha}{4} \\ \frac{\alpha}{4} \end{matrix} \right] \beta L^{\frac{\alpha}{2}} \quad 3 < \alpha < 4. \tag{2.87}$$

In order to generalize $\sigma_\chi^2$ for various system and atmospheric conditions, we can multiply Eq. (2.87) by $\rho_o^{\alpha-2} / \rho_o^{\alpha-2}$ and rearrange the terms to yield

$$\sigma_\chi^2 = \frac{2^{\frac{\alpha-6}{2}} c_1 \pi^{1/2} k^{\frac{2-\alpha}{2}} L^{\frac{\alpha-2}{2}}}{\alpha \rho_o^{\alpha-2}} \Gamma \left[ \begin{matrix} \frac{2-\alpha}{4} & \frac{\alpha}{2} \\ \frac{\alpha}{4} & \frac{2-\alpha}{2} \end{matrix} \right]. \tag{2.88}$$

Define the Fresnel number

$$FN = \sqrt{\lambda L}, \tag{2.89}$$

where $\lambda$ is the wavelength of the beam and $L$ is the length of the optical path. Substituting the definition of Fresnel number into Eq. (2.88) yields

$$\sigma_\chi^2 = \frac{c_1 \pi^{\frac{3-\alpha}{2}}}{4\alpha} \left(\frac{FN}{\rho_o}\right)^{\alpha-2} \Gamma \begin{bmatrix} \frac{2-\alpha}{4} & \frac{\alpha}{2} \\ \frac{\alpha}{4} & \frac{2-\alpha}{2} \end{bmatrix}. \tag{2.90}$$

Figure (2.3) is a plot of the log amplitude variance as a function of power law normalized by $(FN/\rho_o)^{\alpha-2}$. Care must be used in interpreting this plot. Remember

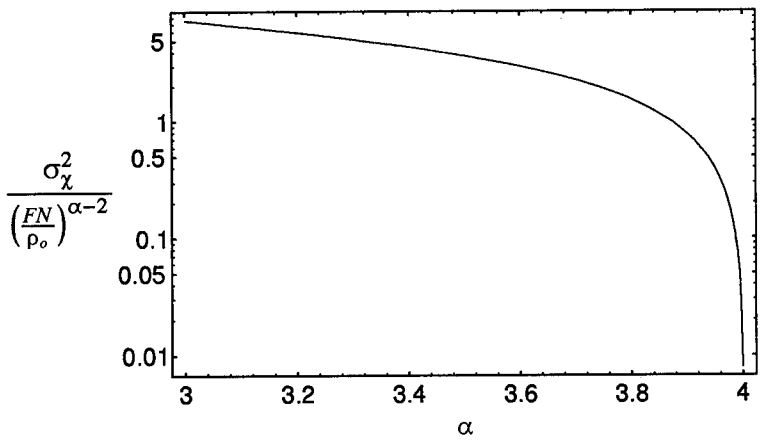


Figure 2.3 The log amplitude variance $\sigma_\chi^2$ as a function of $\alpha$ for normalized by $(FN/\rho_o)^{\alpha-2}$.

for constant turbulence and path conditions $\rho_o$ varies considerably with $\alpha$ (See Fig (2.2)). A key observation can be made at this point. When the spectrum contains fewer eddies of high wavenumber, corresponding to higher power laws ($\alpha \rightarrow 4$), scintillation effects are reduced. This means phase effects dominate as $\alpha \rightarrow 4$, supporting the conclusions of Heidbreder. Figure (2.4) contains plots of the minimum

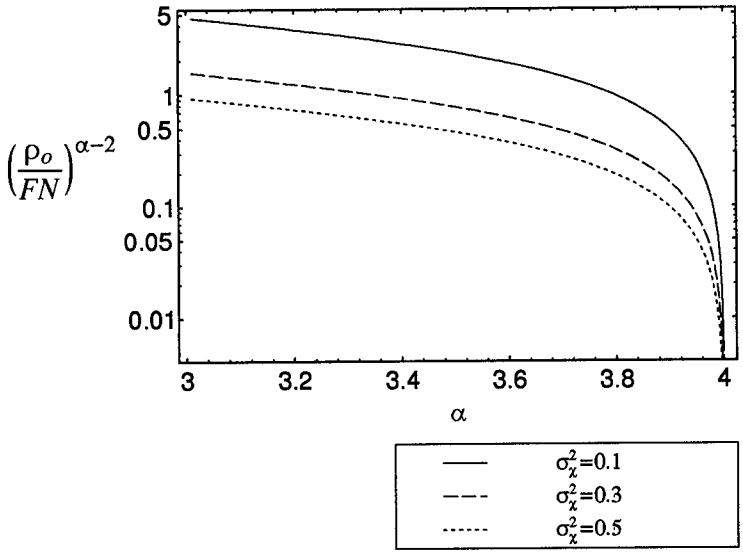


Figure 2.4 The minimum $\rho_o$ normalized by Fresnel number $FN$ for the conditions where $\sigma_\chi^2 = 0.1, 0.3, 0.5$.

$(\rho_o/FN)^{\alpha-2}$ which can be examined using this theory for various values of $\sigma_\chi^2$. One can reject errors due to multiple scattering effects by restricting use of the theory presented in this thesis to the areas above the curves. The area below the curves is considered "strong" turbulence and the theory presented here no longer applies.

# *III. The Extended Huygens-Fresnel Principle*

In this chapter, the extended Huygens-Fresnel principle is used to derive the mutual coherence function for an arbitrary wave in a vacuum and in turbulence. Once the MCF for an arbitrary wave in turbulence is found, it is a simple matter to determine the intensity at any point in the observation plane. The on-axis intensity is of particular interest, because it allows one to easily generate a useful figure-of-merit; the Strehl ratio ($\mathcal{SR}$). The Strehl ratio can be shown to be the ratio of the on-axis intensity of a laser beam in turbulence to that of the laser beam in a vacuum. Thus, the Strehl ratio provides a useful metric for examining the impacts of turbulence on laser beam propagation. In this chapter, the general equations for the MCF and intensities are derived. In Chapter 4, the equations for the on-axis intensity of a general wave are used to calculate the Strehl ratio of a focussed constant amplitude beam.

## *3.1 The Mutual Coherence Function for Quasimonochromatic Waves in a Vacuum*

Following the approach of Lutomirski and Buser [17], the $MCF$ for quasi-monochromatic light is defined as

$$MCF(\mathbf{p_1}, \mathbf{p_2}) = \langle U(x_1, y_1) U^*(x_2, y_2) \rangle \,, \tag{3.1}$$

where $\mathbf{p_1}$ and $\mathbf{p_2}$ are points in the observation plane, $(x_1, y_1)$ and $(x_2, y_2)$ are the $x$ and $y$ coordinates of $\mathbf{p_1}$ and $\mathbf{p_2}$ and the angle brackets denote the statistical expectation operator. Figure (3.1) shows the geometry of the propagation scenario. From the Huygens-Fresnel principle

$$U(x, y) = \frac{-jk}{2\pi} \iint G(x, y, \xi, \eta) U_A(\xi, \eta) \mathrm{d}\xi \mathrm{d}\eta, \tag{3.2}$$

where $\xi$ and $\eta$ are the coordinates of a point in the source plane and the Green's function for propagation of a spherical wave is

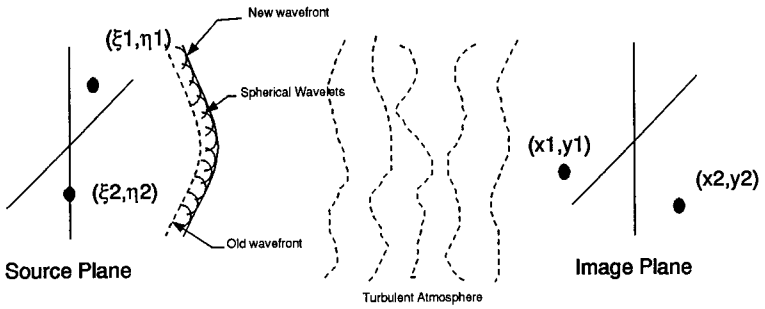


Figure 3.1 A wave propagating from the $(\xi, \eta)$ plane to the $(x, y)$ plane, using the Huygens-Fresnel principle. The primary wavefront is the summation of the envelopes of spherical wavelets whose centers where located on an earlier wavefront.

$$G(x, y, \xi, \eta) = \frac{\exp\left[jk((x-\xi)^2 + (y-\eta)^2 + z^2)^{1/2}\right]}{((x-\xi)^2 + (y-\eta)^2 + z^2))^{1/2}}. \tag{3.3}$$

The integrals in Eq. (3.3) are evaluated over the source aperture. Using the paraxial approximation ($z^2 >> (x-\xi)^2 + (y-\eta)^2$), the numerator of Eq. (3.3) is approximated by

$$\exp\left[jk\left((x-\xi)^2 + (y-\eta)^2 + z^2\right)^{1/2}\right] \rightarrow \exp\left[jk\left(\frac{(x-\xi)^2 + (y-\eta)^2}{2z} + z\right)\right] \tag{3.4}$$

and the denominator by

$$\left((x-\xi)^2 + (y-\eta)^2 + z^2\right)^{1/2} \rightarrow z. \tag{3.5}$$

Substituting Eqs. (3.4) and (3.5) into Eq. (3.2) yields,

$$U(x, y) = \frac{-jk}{2\pi z} \exp[jkz] \iint \exp\left[jk\left(\frac{(x-\xi)^2 + (y-\eta)^2}{2z}\right)\right] U_A(\xi, \eta) \mathrm{d}\xi \mathrm{d}\eta. \tag{3.6}$$

Expanding the terms of the exponential and rearranging, the field is

$$U(x,y) = \frac{-jk}{2\pi z}\exp[jkz]\exp\left[\frac{jk}{2z}(x^2+y^2)\right] \times \iint \exp\left[\frac{jk}{2z}(\xi^2+\eta^2)\right]\exp\left[\frac{-jk}{z}(x\xi+y\eta)\right]U_A(\xi,\eta)\mathrm{d}\xi\mathrm{d}\eta. \quad (3.7)$$

Eq. (3.7) is the standard Fresnel diffraction formula. Substituting Eq. (3.7) into the definition of the MCF, Eq. (3.1), yields

$$MCF(x_1,y_1;x_2,y_2,z) = \left\langle (\frac{k}{2\pi z})^2 \exp\left[\frac{jk}{2z}(x_1^2+y_1^2)\right]\exp\left[\frac{-jk}{2z}(x_2^2+y_2^2)\right] \times \iint \exp\left[\frac{jk}{2z}(\xi_1^2+\eta_1^2)\right]\exp\left[\frac{-jk}{z}(x_1\xi_1+y_1\eta_1)\right]U_A(\xi_1,\eta_1)\mathrm{d}\xi_1\mathrm{d}\eta_1 \times \iint \exp\left[\frac{-jk}{2z}(\xi_2^2+\eta_2^2)\right]\exp\left[\frac{jk}{z}(x_2\xi_2+y_2\eta_2)\right]U_A^*(\xi_2,\eta_2)\mathrm{d}\xi_2\mathrm{d}\eta_2\right\rangle. \quad (3.8)$$

Since the wave is propagating in a deterministic fashion, the expectation operator can be neglected and the MCF for a coherent wave in a vacuum is

$$MCF(x_1,y_1;x_2,y_2,z) = (\frac{k}{2\pi z})^2 \exp\left[\frac{jk}{2z}(x_1^2+y_1^2)-(x_2^2+y_2^2)\right] \times \iiint\!\!\iint \exp\left[\frac{jk}{2z}((\xi_1^2+\eta_1^2)-(\xi_2^2+\eta_2^2))\right] \times \exp\left[\frac{-jk}{z}(x_1\xi_1+y_1\eta_1+x_2\xi_2+y_2\eta_2)\right] \times U_A(\xi_1,\eta_1)U_A^*(\xi_2,\eta_2)\mathrm{d}\xi_1\mathrm{d}\eta_1\mathrm{d}\xi_2\mathrm{d}\eta_2. \quad (3.9)$$

By defining

$$\psi = \exp\left[\frac{jk}{2z}(x_1^2+y_1^2)-(x_2^2+y_2^2)\right], \quad (3.10)$$

the MCF for a quasimonochromatic wave propagating in a vacuum is

$$
\begin{aligned}
&MCF(x_1, y_1; x_2, y_2, z) = \\
&\quad (\frac{k}{2\pi z})^2 \psi \iiiint \exp\left[\frac{jk}{2z}((\xi_1^2 + \eta_1^2) - (\xi_2^2 + \eta_2^2))\right] \\
&\quad \times \exp\left[\frac{-jk}{z}(x_1\xi_1 + y_1\eta_1 + x_2\xi_2 + y_2\eta_2)\right] \\
&\quad \times U_A(\xi_1, \eta_1) U_A^*(\xi_2, \eta_2) \mathrm{d}\xi_1 \mathrm{d}\eta_1 \mathrm{d}\xi_2 \mathrm{d}\eta_2. \qquad (3.11)
\end{aligned}
$$

*3.1.1 The irradiance of a quasimonochromatic wave in a vacuum.* The irradiance at a point $(x_1, y_1)$ can be determined from the MCF by letting $x_2 \rightarrow x_1$ and $y_2 \rightarrow y_1$ in Eq. (3.11),

$$
\begin{aligned}
&I(x_1, y_1, z) = MCF(x_1, y_1; x_1, y_1, z) = \\
&\quad (\frac{k}{2\pi z})^2 \iiiint \exp\left[\frac{jk}{2z}((\xi_1^2 + \eta_1^2) - (\xi_2^2 + \eta_2^2))\right] \\
&\quad \times \exp\left[\frac{-jk}{z}(x_1\xi_1 + y_1\eta_1 + x_1\xi_2 + y_1\eta_2)\right] \\
&\quad \times U_A(\xi_1, \eta_1) U_A^*(\xi_2, \eta_2) \mathrm{d}\xi_1 \mathrm{d}\eta_1 \mathrm{d}\xi_2 \mathrm{d}\eta_2. \qquad (3.12)
\end{aligned}
$$

If we consider only the on-axis irradiance $x_1 \rightarrow 0$ and $y_1 \rightarrow 0$, Eq. (3.12) becomes

$$
\begin{aligned}
&I(0, 0, z) = \\
&\quad (\frac{k}{2\pi z})^2 \iiiint \exp\left[\frac{jk}{2z}((\xi_1^2 + \eta_1^2) - (\xi_2^2 + \eta_2^2))\right] \\
&\quad \times U_A(\xi_1, \eta_1) U_A^*(\xi_2, \eta_2) \mathrm{d}\xi_1 \mathrm{d}\eta_1 \mathrm{d}\xi_2 \mathrm{d}\eta_2. \qquad (3.13)
\end{aligned}
$$

Equation (3.13) is a separable integral,

$$I(0,0,z) =$$
$$(\frac{k}{2\pi z})^2 \iint \exp\left[\frac{jk}{2z}(\xi_1^2+\eta_1^2)\right] U_A(\xi_1,\eta_1)\mathrm{d}\xi_1\mathrm{d}\eta_1$$
$$\times \iint \exp\left[\frac{-jk}{2z}(\xi_2^2+\eta_2^2)\right] U_A^*(\xi_2,\eta_2)\mathrm{d}\xi_2\mathrm{d}\eta_2. \qquad (3.14)$$

## *3.2 The Mutual Coherence Function for Quasimonochromatic Waves in Non-Kolmogorov Turbulence*

In this section the MCF for an arbitrary wave in non-Kolmogorov turbulence is derived. The derivation proceeds as in the last section, except for the substitution of a different Green's function.

The $MCF$ for quasimonochromatic light is defined as

$$MCF(\mathbf{p_1},\mathbf{p_2}) = \langle U(x_1,y_1)U^*(x_2,y_2)\rangle, \qquad (3.15)$$

where $\mathbf{p_1}$ and $\mathbf{p_2}$ are points in the observation plane, and $(x_1,y_1)$ and $(x_2,y_2)$ are the $x$ and $y$ coordinates of $\mathbf{p_1}$ and $\mathbf{p_2}$.

From the Huygens-Fresnel principle:

$$U(x,y) = \frac{-jk}{2\pi}\iint G(x,y,\xi,\eta)U_A(\xi,\eta)\mathrm{d}\xi\mathrm{d}\eta, \qquad (3.16)$$

where $\xi$ and $\eta$ are the coordinates of a point in the source plane and $G(x,y,\xi,\eta)$ is the Green's function for propagation in turbulence. The integrals are again taken over the source aperture. If we define $G'(x,y,\xi,\eta)$ as the ratio of $G(x,y,\xi,\eta)$ to its value in the absence of turbulence [17],

$$G(x,y,\xi,\eta) = \frac{\exp[jk((x-\xi)^2+(y-\eta)^2+z^2)^{1/2}]}{((x-\xi)^2+(y-\eta)^2+z^2)^{1/2}} G'(x,y,\xi,\eta). \qquad (3.17)$$

Applying the paraxial approximation and substituting Eq. (3.17) into Eq. (3.16) yields

$$U(x,y) = \frac{-jk}{2\pi z}\exp[jkz] \times \iint G'(x,y,\xi,\eta)\exp\left[jk(\frac{(x-\xi)^2+(y-\eta)^2}{2z})\right]U_A(\xi,\eta)\mathrm{d}\xi\mathrm{d}\eta. \quad (3.18)$$

Substituting Eq. (3.18) into Eq. (3.15),

$$\begin{aligned} MCF(x_1,y_1;x_2,y_2,z) = & \\ & \left\langle (\frac{k}{2\pi z})^2 \iiint\!\!\iint G'(x_1,y_1,\xi_1,\eta_1)G'^*(x_2,y_2,\xi_2,\eta_2) \right. \\ & \times \exp\left[jk\left(\frac{(x_1-\xi_1)^2+(y_1-\eta_1)^2}{2z}\right)\right] \\ & \times \exp\left[-jk\left(\frac{(x_2-\xi_2)^2+(y_2-\eta_2)^2}{2z}\right)\right] \\ & \left. \times U_A(\xi_1,\eta_1)U_A^*(\xi_2,\eta_2)\mathrm{d}\xi_1\mathrm{d}\eta_1\mathrm{d}\xi_2\mathrm{d}\eta_2 \right\rangle. \end{aligned} \quad (3.19)$$

Interchanging the order of integration and expectation and defining

$$H(x_1,y_1,\xi_1,\eta_1,x_2,y_2,\xi_2,\eta_2,z) = \langle G'(x_1,y_1,\xi_1,\eta_1,z)G'^*(x_2,y_2,\xi_2,\eta_2,z)\rangle, \quad (3.20)$$

yields

$$\begin{aligned} MCF(x_1,y_1;x_2,y_2,z) = & \\ & (\frac{k}{2\pi z})^2 \iiint\!\!\iint H(x_1,y_1,\xi_1,\eta_1,x_2,y_2,\xi_2,\eta_2,z) \\ & \times \exp\left[\frac{jk}{2z}((x_1-\xi_1)^2+(y_1-\eta_1)^2)-((x_2-\xi_2)^2+(y_2-\eta_2)^2))\right] \\ & \times U_A(\xi_1,\eta_1)U_A^*(\xi_2,\eta_2)\mathrm{d}\xi_1\mathrm{d}\eta_1\mathrm{d}\xi_2\mathrm{d}\eta_2. \end{aligned} \quad (3.21)$$

Expanding the terms in the exponential and rearranging, Eq.(3.21) becomes

$$\begin{aligned} MCF(x_1, y_1; x_2, y_2, z) = \\ &(\frac{k}{2\pi z})^2 \exp\left[\frac{jk}{2z}(x_1^2 + y_1^2) - (x_2^2 + y_2^2)\right] \\ &\times \iiiint H(x_1, y_1, \xi_1, \eta_1, x_2, y_2, \xi_2, \eta_2, z) \\ &\times \exp\left[\frac{jk}{2z}((\xi_1^2 + \eta_1^2) - (\xi_2^2 + \eta_2^2) + 2x_2\xi_2 - 2x_1\xi_1 + 2y_2\eta_2 - 2y_1\eta_1)\right] \\ &\times U_A(\xi_1, \eta_1) U_A^*(\xi_2, \eta_2) \mathrm{d}\xi_1 \mathrm{d}\eta_1 \mathrm{d}\xi_2 \mathrm{d}\eta_2. \end{aligned} \tag{3.22}$$

By defining

$$\psi = \exp\left[\frac{jk}{2z}(x_1^2 + y_1^2) - (x_2^2 + y_2^2)\right], \tag{3.23}$$

the MCF of a quasimonochromatic wave in non-Kolmogorov turbulence is

$$\begin{aligned} MCF(x_1, y_1; x_2, y_2, z) = \\ &(\frac{k}{2\pi z})^2 \psi \iiiint H(x_1, y_1, \xi_1, \eta_1, x_2, y_2, \xi_2, \eta_2, z) \\ &\times \exp\left[\frac{jk}{2z}((\xi_1^2 + \eta_1^2) - (\xi_2^2 + \eta_2^2) + 2x_2\xi_2 - 2x_1\xi_1 + 2y_2\eta_2 - 2y_1\eta_1)\right] \\ &\times U_A(\xi_1, \eta_1) U_A^*(\xi_2, \eta_2) \mathrm{d}\xi_1 \mathrm{d}\eta_1 \mathrm{d}\xi_2 \mathrm{d}\eta_2. \end{aligned} \tag{3.24}$$

Equation (3.24) is the major result of this chapter. We will see in the next chapter that $H(x_1, y_1, \xi_1, \eta_1, x_2, y_2, \xi_2, \eta_2, z)$ takes the form

$$H(x_1, y_1, \xi_1, \eta_1, x_2, y_2, \xi_2, \eta_2, z) = \exp\left[-\frac{1}{2} D_w(\rho)\right] \tag{3.25}$$

where $D_w(\rho)$ is the wave structure function derived in Chapter 2 and $\rho$ is the geometric separation of the points $(\xi_1, \eta_1)$ and $(\xi_2, \eta_2)$ in the source plane.

*3.2.1 The irradiance of a quasimonochromatic wave in non-Kolmogorov turbulence.* The irradiance at a point $(x, y)$ in the observation plane can be deter-

mined by letting $x_2 \to x_1$ and $y_2 \to y_1$ in Eq. (3.24),

$$
\begin{aligned}
&I(x_1, y_1, z) = \\
&\quad (\frac{k}{2\pi z})^2 \iiiint H(x_1, y_1, \xi_1, \eta_1, x_2, y_2, \xi_2, \eta_2, z) \\
&\quad \times \exp\left[\frac{jk}{2z}((\xi_1^2 + \eta_1^2) - (\xi_2^2 + \eta_2^2) + 2x_1\xi_2 - 2x_1\xi_1 + 2y_1\eta_2 - 2y_1\eta_1)\right] \\
&\quad \times U_A(\xi_1, \eta_1) U_A^*(\xi_2, \eta_2) \mathrm{d}\xi_1 \mathrm{d}\eta_1 \mathrm{d}\xi_2 \mathrm{d}\eta_2. \qquad (3.26)
\end{aligned}
$$

Considering only the on-axis irradiance, let $x_1 \to 0$ and $y_1 \to 0$, then

$$
\begin{aligned}
&I(0, 0, z) = \\
&\quad (\frac{k}{2\pi z})^2 \iiiint H(x_1, y_1, \xi_1, \eta_1, x_2, y_2, \xi_2, \eta_2, z) \\
&\quad \times \exp\left[\frac{jk}{2z}((\xi_1^2 + \eta_1^2) - (\xi_2^2 + \eta_2^2)\right] \\
&\quad \times U_A(\xi_1, \eta_1) U_A^*(\xi_2, \eta_2) \mathrm{d}\xi_1 \mathrm{d}\eta_1 \mathrm{d}\xi_2 \mathrm{d}\eta_2. \qquad (3.27)
\end{aligned}
$$

We will use the Eqs. (3.14) and (3.27) for the on-axis intensities in vacuum and in turbulence extensively in Chapter 4 to compute the Strehl ratio of a focussed, constant amplitude beam.

# *IV. The Strehl Ratio of a Laser Beam in Non-Kolmogorov Atmospheric Turbulence*

In order to calculate the impact turbulence has on laser beam propagation, one can use many different performance metrics. A common performance metric is the Strehl ratio. The Strehl ratio is defined as

$$\mathcal{SR} = \frac{I(0,0)_{\text{in turbulence}}}{I(0,0)_{\text{in vacuum}}}, \tag{4.1}$$

where $I(0,0)$ is the on-axis irradiance.

In this chapter the on-axis irradiances of a wave in a vacuum and in turbulence, hence the Strehl ratio, are calculated using the mutual coherence function (MCF) derived in Chapter 3 and the wave structure function $D_w(\rho)$ derived in Chapter 2. In Section 4.2, the Strehl ratio as a function of power law $\alpha$ is plotted for constant values of the generalized coherence diameter $\rho_o$. Next, the asymptotic behavior of Fried's resolution metric $\mathcal{R}/\mathcal{R}_{\max}$ is examined [8]. It is from this behavior that the constant $c_1$ in Eq. (2.74) is determined. Additionally, $\mathcal{R}/\mathcal{R}_{\max}$ is shown to be the Strehl ratio multiplied by $(D/\rho_o)^2$ or

$$\frac{\mathcal{R}}{\mathcal{R}_{\max}} = \mathcal{SR}\left(\frac{D}{\rho_o}\right)^2. \tag{4.2}$$

Equation (4.2) is plotted for various power laws in Section 4.3.

Great care must be used in finding a reasonable basis on which to compare the Strehl ratios of beams propagating through different power spectra. Consider the two power spectra

$$\Phi_{n_1}(\kappa, \alpha_1, \beta_o) = a(\alpha_1)\beta_o\kappa^{-\alpha_1} \quad \Phi_{n_2}(\kappa, \alpha_2, \beta_o) = a(\alpha_2)\beta_o\kappa^{-\alpha_2}. \tag{4.3}$$

If $\alpha_1$ does not equal $\alpha_2$, then the power in any finite bandwidth of the two spectra will not be equal. Thus, in a plot of the Strehl ratio as a function of the power law $\alpha$, it is difficult to separate the effects of the total power in the turbulence from how that power is weighted in spatial wavenumber. We shall see in this chapter that, the choice of basis for comparing different power laws greatly impacts the trends of Strehl ratio.

The latter sections of this chapter contain plots of the Strehl ratio as a function of the power law under different bases of comparison. Ultimately, any individual basis boils down to a rule on how $\beta L$ is chosen as the power law varies. First, $\beta L$ is fixed and the power law $\alpha$ is allowed to vary over the domain, $3 < \alpha < 4$. Following this comparison, $\beta L$ is chosen such that the power spectra are constant at a specific wavenumber $\kappa_o$. Next, $\beta L$ is chosen to be such that, the power over a finite bandwidth is constant as the power law varies. We will see that the results of the two previous comparisons are similar. Next, $\beta L$ is chosen such that, the piston-removed wave variance $\sigma^2_{w_{-p}}$ over the receiver aperture is constant as the power law varies.

## *4.1 Strehl Ratio for a Focused Constant-Amplitude Beam*

In this section an equation for the Strehl ratio is derived using the wave structure function derived in Chapter 2 and the extended Huygens-Fresnel principle described in Chapter 3. First, let the field in the source aperture be a constant-amplitude beam focussed at distance $z$,

$$U(\xi, \eta) = \exp\left[\frac{jk}{2z}(\xi^2 + \eta^2)\right]. \tag{4.4}$$

*4.1.1 Evaluation of the on-axis irradiance in turbulence.* Substituting Eq. (4.4) into Eq. (3.27) yields

$$I(0,0,z)_{\text{in turbulence}} = \left(\frac{k}{2\pi z}\right)^2 \iiiint H(x_1, y_1, \xi_1, \eta_1, x_2, y_2, \xi_2, \eta_2, z) \mathrm{d}\xi_1 \mathrm{d}\eta_1 \mathrm{d}\xi_2 \mathrm{d}\eta_2. \tag{4.5}$$

Lutomirski and Buser [17] show that $H(x_1, y_1, \xi_1, \eta_1, x_2, y_2, \xi_2, \eta_2, z)$ in Eqs. (3.24), (3.26) and (3.27) is

$$H(x_1, y_1, \xi_1, \eta_1, x_2, y_2, \xi_2, \eta_2, z) = \exp\left[-\frac{1}{2} D_w(((\xi_1 - \xi_2)^2 + (\eta_1 - \eta_2)^2)^{1/2})\right], \tag{4.6}$$

where $D_w$ is the spherical wave structure function derived in Chapter 2 and $\rho = ((\xi_1 - \xi_2)^2 + (\eta_1 - \eta_2)^2)^{1/2}$ is the geometric distance between two points in the source plane. Substituting Eq. (4.6) into Eq. (4.5) yields

$$I(0,0,z)_{\text{in turbulence}} = \left(\frac{k}{2\pi z}\right)^2 \iiiint \exp\left[-\frac{1}{2} D_w(\rho)\right] \mathrm{d}\xi_1 \mathrm{d}\eta_1 \mathrm{d}\xi_2 \mathrm{d}\eta_2. \tag{4.7}$$

Equation (4.7) is a four dimensional integral over the source aperture. We define the circular aperture function

$$W(\xi_1 \hat{\xi} + \eta_1 \hat{\eta}) = \begin{cases} 1 & |\xi_1 \hat{\xi} + \eta_1 \hat{\eta}| \leq D/2 \\ 0 & \text{otherwise,} \end{cases} \tag{4.8}$$

where $\hat{\xi}$ and $\hat{\eta}$ are unit vectors in the source plane and $D$ is the aperture diameter. Substituting Eq. (4.8) into Eq. (4.7) yields

$$I(0,0,z)_{\text{in turbulence}} = \left(\frac{k}{2\pi z}\right)^2 \int_{-\infty}^{\infty}\int_{-\infty}^{\infty}\int_{-\infty}^{\infty}\int_{-\infty}^{\infty} W(\xi_1 \hat{\xi} + \eta_1 \hat{\eta}) W(\xi_2 \hat{\xi} + \eta_2 \hat{\eta}) \times \exp\left[-\frac{1}{2} D_w(\rho)\right] \mathrm{d}\xi_1 \mathrm{d}\eta_1 \mathrm{d}\xi_2 \mathrm{d}\eta_2. \tag{4.9}$$

Equation (4.9) is converted to vector notation with the following change of variables

$$\begin{aligned} \vec{\mathbf{r}} &= (\xi_1 - \xi_2)\hat{\xi} + (\eta_1 - \eta_2)\hat{\eta} \qquad & \mathrm{d}\vec{\mathbf{r}} &= \mathrm{d}\xi_1 \mathrm{d}\eta_1 \\ \vec{\mathbf{r}}' &= \tfrac{1}{2}((\xi_1 + \xi_2)\hat{\xi} + (\eta_1 + \eta_2)\hat{\eta}) & \mathrm{d}\vec{\mathbf{r}}' &= \mathrm{d}\xi_2 \mathrm{d}\eta_2, \end{aligned} \tag{4.10}$$

thus,

$$\vec{\mathbf{r}}' + \tfrac{1}{2}(\vec{\mathbf{r}}) = \xi_1\hat{\xi} + \eta_1\hat{\eta} \quad \vec{\mathbf{r}}' - \tfrac{1}{2}(\vec{\mathbf{r}}) = \xi_2\hat{\xi} + \eta_2\hat{\eta}. \tag{4.11}$$

Substituting Eqs. (4.10) and (4.11) into Eq. (4.9) yields

$$\begin{aligned} &I(0,0,z)_{\text{in turbulence}} = \\ &\quad (\frac{k}{2\pi z})^2 \int_{-\infty}^{\infty}\int_{-\infty}^{\infty} W(\vec{\mathbf{r}}' + \frac{1}{2}(\vec{\mathbf{r}}))W(\vec{\mathbf{r}}' - \frac{1}{2}(\vec{\mathbf{r}})) \\ &\quad \times \exp\left[-\frac{1}{2}D_w(|\vec{\mathbf{r}}|)\right] \mathrm{d}\vec{\mathbf{r}}\mathrm{d}\vec{\mathbf{r}}'. \end{aligned} \tag{4.12}$$

Because $W(\vec{\mathbf{r}}' + \frac{1}{2}(\vec{\mathbf{r}}))$ and $W(\vec{\mathbf{r}}' - \frac{1}{2}(\vec{\mathbf{r}}))$ represent circular apertures they are independent of orientation in the source plane, thus, Eq. (4.12) can be written as

$$\begin{aligned} &I(0,0,z)_{\text{in turbulence}} = \\ &\quad (\frac{k}{2\pi z})^2 \int_{-\infty}^{\infty}\int_{-\infty}^{\infty} W(|\vec{\mathbf{r}}' + \frac{1}{2}(\vec{\mathbf{r}})|)W(|\vec{\mathbf{r}}' - \frac{1}{2}(\vec{\mathbf{r}})|) \\ &\quad \times \exp\left[-\frac{1}{2}D_w(|\vec{\mathbf{r}}|)\right] \mathrm{d}\vec{\mathbf{r}}\mathrm{d}\vec{\mathbf{r}}'. \end{aligned} \tag{4.13}$$

The integral over $\vec{\mathbf{r}}'$ can be evaluated in closed form [9],

$$\int W(|\vec{\mathbf{r}}' + \frac{1}{2}(\vec{\mathbf{r}})|)W(|\vec{\mathbf{r}}' - \frac{1}{2}(\vec{\mathbf{r}})|)\mathrm{d}\vec{\mathbf{r}}' = \tag{4.14}$$

$$\begin{cases} \frac{1}{2}\left[D^2\cos^{-1}(\frac{|\vec{\mathbf{r}}|}{D}) - |\vec{\mathbf{r}}|(D^2 - |\vec{\mathbf{r}}|^2)^{1/2}\right] & |\vec{\mathbf{r}}| \le D \\ 0 & \text{otherwise,} \end{cases}$$

where $D$ is the diameter of the aperture. Substituting Eq. (4.14) into Eq. (4.13) yields

$$I(0,0,z)_{\text{in turbulence}} = \left(\frac{k}{2\pi z}\right)^2 \int_{-\infty}^{\infty} \frac{1}{2}\left[D^2 \cos^{-1}\left(\frac{|\vec{\mathbf{r}}|}{D}\right) - |\vec{\mathbf{r}}|(D^2 - |\vec{\mathbf{r}}|^2)^{1/2}\right] \times \exp\left[-\frac{1}{2}D_w(|\vec{\mathbf{r}}|)\right] \mathrm{d}\vec{\mathbf{r}}. \tag{4.15}$$

Changing to polar coordinates, the on-axis irradiance becomes,

$$I(0,0,z)_{\text{in turbulence}} = \left(\frac{k}{2\pi z}\right)^2 2\pi \int_0^D r K_o(r) \exp\left[-\frac{1}{2}D_w(r)\right] \mathrm{d}r, \tag{4.16}$$

where,

$$K_o(r) = \frac{1}{2}\left[D^2 \cos^{-1}\left(\frac{r}{D}\right) - r(D^2 - r^2)^{1/2}\right]. \tag{4.17}$$

*4.1.2 Evaluation of the on-axis irradiance in a vacuum.* The on-axis irradiance in vacuum is given by Eq. (3.14)

$$I(0,0,z)_{\text{in vacuum}} = \left(\frac{k}{2\pi z}\right)^2 \iint \exp\left[\frac{jk}{2z}(\xi_1^2 + \eta_1^2)\right] U_A(\xi_1,\eta_1) d\xi_1 d\eta_1 \times \iint \exp\left[\frac{-jk}{2z}(\xi_2^2 + \eta_2^2)\right] U_A^*(\xi_2,\eta_2) d\xi_2 d\eta_2. \tag{4.18}$$

Substituting the field (Eq. (4.4)) and the aperture functions (Eq. (4.8)) and evaluating the integrals yields

$$I(0,0,z)_{\text{in vacuum}} = \left(\frac{k}{2\pi z}\right)^2 \pi^2 \left(\frac{D}{2}\right)^4. \tag{4.19}$$

Using the definition of Strehl ratio we obtain

$$\mathcal{SR} = \frac{I(0,0)_{\text{in turbulence}}}{I(0,0)_{\text{in vacuum}}} = \frac{2\pi}{\pi^2\left(\frac{D}{2}\right)^4}\int_0^D rK_o(r)\exp\left[-\frac{1}{2}D_w(r)\right]\mathrm{d}r. \tag{4.20}$$

Equation (4.20) is evaluated numerically in the latter sections of this chapter, as the wave structure function is varied according to a rule on how $\beta L$ is chosen for a particular power law $\alpha$.

## *4.2 Asymptotic Behavior of Fried's Resolution Metric for Non-Kolmogorov Turbulence*

In the previous section, the Strehl ratio was found to be

$$\mathcal{SR} = \frac{I(0,0)_{\text{in turbulence}}}{I(0,0)_{\text{in vacuum}}} = \frac{2\pi}{\pi^2\left(\frac{D}{2}\right)^4}\int_0^D rK_o(r)\exp\left[-\frac{1}{2}D_w(r)\right]\mathrm{d}r. \tag{4.21}$$

Equation (4.21) can be simplified. Making the change of variables

$$\begin{aligned} u &= \frac{r}{D} \qquad r = Du \\ \mathrm{d}u &= \frac{\mathrm{d}r}{D} \quad \mathrm{d}r = D\mathrm{d}u, \end{aligned} \tag{4.22}$$

and substituting Eq. (4.17) into Eq. (4.21) yields

$$\mathcal{SR} = \frac{32}{\pi D^4}\int_0^1 \frac{1}{2}(D^2\cos^{-1}(u) - Du\sqrt{D^2 - D^2u^2})\exp\left[-\frac{1}{2}D_w(Du)\right]D^2u\mathrm{d}u. \tag{4.23}$$

Substituting Eq. (2.74) into Eq. (4.23) and simplifying yields

$$\mathcal{SR} = \frac{32}{\pi}\int_0^1 \frac{1}{2}(\cos^{-1}(u) - u\sqrt{1-u^2})\exp\left[-\frac{1}{2}c_1\left(\frac{D}{\rho_o}u\right)^{\alpha-2}\right]u\mathrm{d}u. \tag{4.24}$$

In order to evaluate Eq. (4.24) we need to choose an appropriate constant $c_1$. This will be done in the same manner as Fried [8]. Fried chose the constant $c_1$ based on

the asymptotic behavior of a performance metric similiar to the Strehl ratio. He called this metric the resolution $\mathcal{R}$. The resolution $\mathcal{R}$ is defined as

$$\mathcal{R} = 2\pi \int_0^\infty \omega H(\omega) \mathrm{d}\omega, \tag{4.25}$$

where $H(\omega)$ is the long exposure optical transfer function (OTF) of an incoherent imaging system in the presence of turbulence. Fried examined the ratio $\mathcal{R}/\mathcal{R}_{max}$, where $\mathcal{R}_{max}$ is defined as the resolution of an imaging system in turbulence with an infinite aperture diameter

$$\mathcal{R}_{max} = \lim_{D\to\infty} \mathcal{R}. \tag{4.26}$$

The ratio of $\mathcal{R}/\mathcal{R}_{max}$ yields an expression similar to Strehl ratio in Eq. (4.24).

$$\mathcal{R}/\mathcal{R}_{max} = \frac{32D^2}{\pi r_o^2} \int_0^1 \frac{1}{2}(\cos^{-1}(u) - u\sqrt{1-u^2}) \exp\left[-\frac{1}{2}c_1 \left(\frac{D}{r_o}u\right)^{5/3}\right] u\mathrm{d}u, \tag{4.27}$$

where $r_o$ is the atmospheric coherence diameter for Kolmogorov turbulence (See Eq. (2.72)) [8]. Thus, Fried's resolution metric $\mathcal{R}/\mathcal{R}_{max}$ for an arbitrary power law can be found by multiplying Eq. (4.24) by $(D/\rho_o)^2$

$$\begin{aligned}\mathcal{R}/\mathcal{R}_{max} &= \mathcal{S}\mathcal{R}(D/\rho_o)^2 = \\ &\frac{32D^2}{\pi\rho_o^2}\int_0^1 \frac{1}{2}(\cos^{-1}(u) - u\sqrt{1-u^2}) \exp\left[-\frac{1}{2}c_1 \left(\frac{D}{\rho_o}u\right)^{\alpha-2}\right] u\mathrm{d}u.\end{aligned} \tag{4.28}$$

To find the constant $c_1$, make the change of variables

$$\begin{aligned} x &= \tfrac{Du}{\rho_o} \qquad u = \tfrac{\rho_o x}{D} \\ \mathrm{d}x &= \tfrac{D\mathrm{d}u}{\rho_o} \quad \mathrm{d}u = \tfrac{\rho_o \mathrm{d}x}{D} \end{aligned}.$$

Thus, Eq. (4.28) becomes

$$\mathcal{R}/\mathcal{R}_{max} =$$
$$\frac{32}{\pi}\int_0^{\frac{D}{\rho_o}}\frac{1}{2}\left(\cos^{-1}\left(\frac{\rho_o x}{D}\right)-\left(\frac{\rho_o x}{D}\right)\sqrt{1-\left(\frac{\rho_o x}{D}\right)^2}\right)$$
$$\times\exp\left[-\frac{1}{2}c_1 x^{\alpha-2}\right]x\mathrm{d}x. \tag{4.29}$$

Let the aperture diameter increase until $D \rightarrow \infty$, thus $\frac{1}{2}\left(\cos^{-1}(\rho_o x/D)-(\rho_o x/D)\sqrt{1-(\rho_o x/D)^2}\right)\rightarrow \pi/4$ and Eq. (4.28) takes the form

$$\lim_{D\rightarrow\infty}\{\mathcal{R}/\mathcal{R}_{max}\} = 8\int_0^{\infty}\exp\left[-\frac{1}{2}c_1 x^{\alpha-2}\right]x\mathrm{d}x. \tag{4.30}$$

By making another change of variables

$$v=\frac{c_1}{2}x^{\alpha-2} \qquad x=\left(\frac{2v}{c_1}\right)^{\frac{1}{\alpha-2}} \tag{4.31}$$
$$\mathrm{d}v=\frac{c_1(\alpha-2)}{2}x^{\alpha-3}\mathrm{d}x \quad \mathrm{d}x=\frac{1}{\alpha-2}\left(\frac{2}{c_1}\right)^{\frac{1}{\alpha-2}}v^{\frac{1}{\alpha-2}-1}\mathrm{d}v,$$

Eq. (4.30) reduces to

$$\lim_{D\rightarrow\infty}\{\mathcal{R}/\mathcal{R}_{max}\} = \frac{8}{\alpha-2}\left(\frac{2}{c_1}\right)^{\frac{2}{\alpha-2}}\int_0^{\infty}\exp[-v]v^{\frac{2}{\alpha-2}-1}\mathrm{d}v. \tag{4.32}$$

The integral in Eq. (4.32) can be recognized as $\Gamma[2/\alpha-2]$, thus Eq. (4.32) is

$$\lim_{D\rightarrow\infty}\{\mathcal{R}/\mathcal{R}_{max}\} = \frac{8}{\alpha-2}\left(\frac{2}{c_1}\right)^{\frac{2}{\alpha-2}}\Gamma\left[\frac{2}{\alpha-2}\right]. \tag{4.33}$$

Since $\lim_{D\rightarrow\infty}\{\mathcal{R}/\mathcal{R}_{max}\} = \mathcal{R}_{max}/\mathcal{R}_{max} = 1$ solving for $c_1$ yields

$$c_1 = 2\left(\frac{8}{\alpha-2}\Gamma\left[\frac{2}{\alpha-2}\right]\right)^{\frac{\alpha-2}{2}}. \tag{4.34}$$

If we let $\alpha = 11/3$, $c_1$ reduces to the constant in Fried's structure function

$$c_1 = 2\left(\frac{24}{5}\Gamma\left[\frac{6}{5}\right]\right)^{\frac{5}{6}} \approx 6.88. \tag{4.35}$$

To show the behavior of an imaging system when the aperture size is much smaller than $\rho_o$ let $D/\rho_o \to 0$, the exponential term in Eq. (4.28) goes to 1 and

$$\mathcal{R}/\mathcal{R}_{max} = \frac{32D^2}{\pi\rho_o^2}\int_0^1 \frac{1}{2}(\cos^{-1}(u) - u\sqrt{1-u^2})u\,du. \tag{4.36}$$

Equation (4.36) reduces to

$$\mathcal{R}/\mathcal{R}_{max} = \frac{16}{\pi}\left(\frac{D}{\rho_o}\right)^2\left(\frac{\pi}{8} - \frac{\pi}{16}\right) = \left(\frac{D}{\rho_o}\right)^2. \tag{4.37}$$

Figure (4.1) shows $\mathcal{R}/\mathcal{R}_{max}$ as a function of $D/\rho_o$ for various power laws. Notice the only effect the power law has on $\mathcal{R}/\mathcal{R}_{max}$ is to round off the knee of the curve. This is another result of the definition of $\rho_o$. Remember $\rho_o$ varies greatly with the power law for a constant integrated turbulence strength.

### *4.3 Comparing Strehl Ratios in Arbitrary Power Law Turbulence Spectra when $D/\rho_o$ is Constant*

Figure (4.2) is a plot of the Strehl ratio as a function of the power law $\alpha$ for various values of $D/\rho_o$. The Strehl ratio is computed using Eq. (4.24). Notice that the Strehl ratio does not seem to change appreciably with power law. Remember that for a fixed integrated turbulence strength $\beta L$, $\rho_o$ varies greatly with the power law $\alpha$ (See Fig. (2.2)). Thus, in Figure (4.2) $D$ is varying just as greatly with the power law to maintain a constant ratio of $D/\rho_o$. It is clear that another point of view must be taken to understand how the Strehl ratio varies with power law.

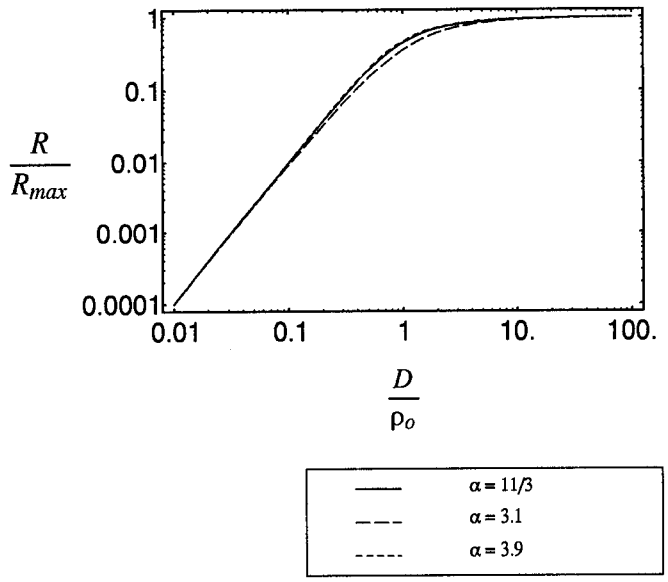


Figure 4.1 $\mathcal{R}/\mathcal{R}_{max}$ as a function of $D/\rho_o$ for various power laws (See Eq. (4.28)).

### *4.4 Comparing Strehl Ratios in Arbitrary Power Law Turbulence Spectra when $\beta L$ is Constant*

The next basis on which to compare Strehl ratios as the power law $\alpha$ varies is to leave $\beta L$ constant. This basis is appropriate for the ARGUS anemometer case where $\beta$ may be estimated correctly, but the uncertainty in the actual value of the power law is large due to the unknown anemometer probe frequency response. Figure (4.3) is a plot of the Strehl ratio as a function of the power law $\alpha$ for a 1 m diameter, circular source aperture. The wavelength is 1.3 microns. Notice Fig. (4.3) follows the same general trends as $\rho_o$ in Fig. (2.2). We would expect this behavior since $\beta L$ is fixed in both cases. The Strehl ratio approaches 1 when $\alpha = 3$, because as was shown in Chapter 2, the turbulence vanishes. The Strehl ratio approaches 0 when $\alpha = 4$ because the abberations induced on the optical wave are pure random tilts in

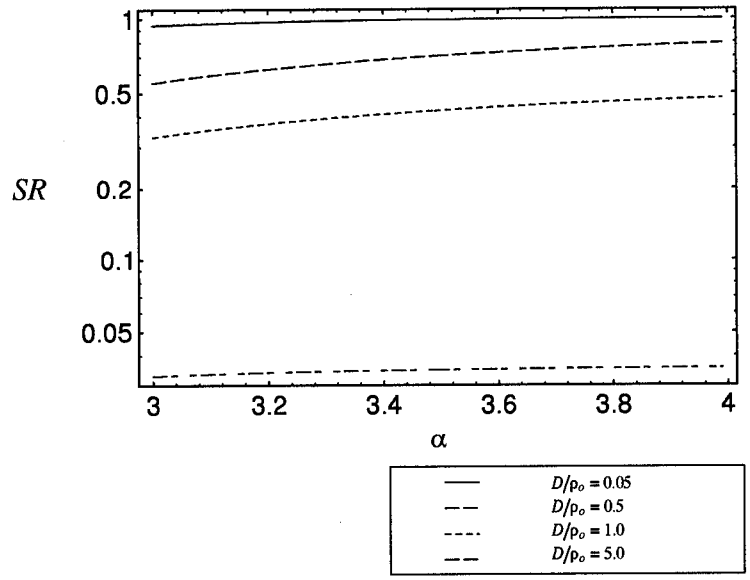


Figure 4.2 The Strehl ratio as a function of $\alpha$ (See Eq. (4.24). $D/\rho_o$ is fixed at the value specified in the legend.

the source plane. These random tilts cause a greatly increased long exposure spot size due to beam wander. Note: this interpretation is only valid if inner and outer scale effects are neglected.

### *4.5 Comparing Strehl Ratios in Arbitrary Power Law Turbulence Spectra when $\beta L$ is such that $a(\alpha)\beta L\kappa_o^{-\alpha}$ is Constant*

In this comparison $\beta L$ is chosen such that the power spectrum for each arbitrary power law at a specific wavenumber $\kappa_o$ is constant. $\beta L$ is found using the following relation,

$$a(\alpha)\beta L\kappa_o^{-\alpha} - a(11/3)C_n^2 L\kappa_o^{-11/3} = 0. \tag{4.38}$$

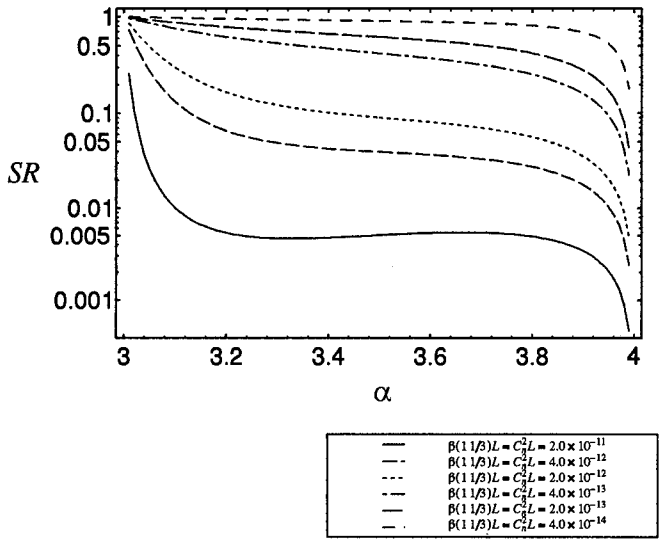


Figure 4.3 The Strehl ratio as a function of $\alpha$. $\beta L$ is constant and fixed at the value specified in the legend. The source aperture diameter $D$ is 1.0 m. The wavelength is 1.3 microns.

Solving Eq. (4.38) for $\beta L$ yields

$$\beta L = \frac{a(11/3)}{a(\alpha)} C_n^2 L \kappa_o^{\alpha - 11/3}. \tag{4.39}$$

This basis is also appropriate for the ARGUS data, where the frequency response of the anemometer probes may not corrupt the measurement of $\beta$ in certain wavenumber ranges. Figure (4.4) is a plot of the Strehl ratio as a function of the power law $\alpha$ for a 1 m diameter, circular source aperture. The wavenumber at which the spectra are equal is $\kappa_o = 1\text{m}^{-1}$. The wavelength is 1.3 microns. One can see from Figure (4.4) that the constraint forces $\beta L$ to be large when $\alpha = 3$, thus $\rho_o$ and the Strehl ratio are small. As the power law increases, the constraint forces $\beta L$ to become smaller until the effect of pure tilt dominates when $\alpha \rightarrow 4$.

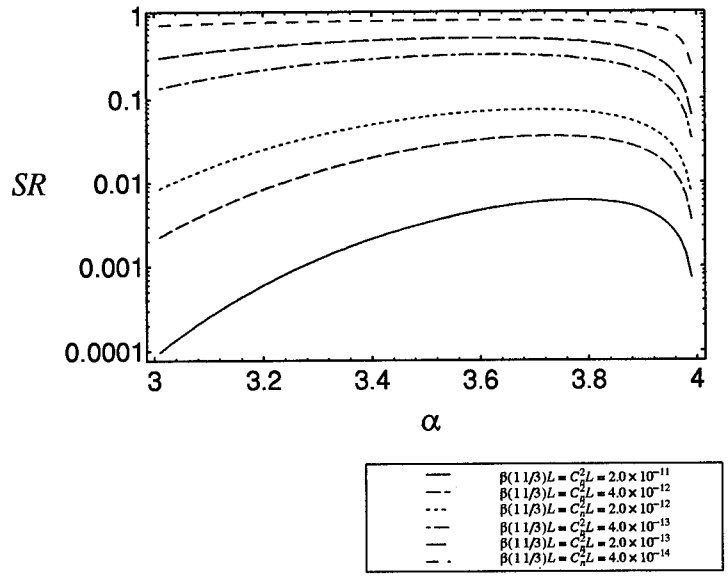


Figure 4.4 The Strehl ratio as a function of $\alpha$. $\beta L$ is chosen such that Eq. (4.39) is satisfied for the values of $C_n^2 L$ specified in the legend. The source aperture diameter $D$ is 1.0 m. The wavelength is 1.3 microns. The wavenumber at which the spectra are equal is $\kappa_o = 1\mathrm{m}^{-1}$.

### *4.6 Comparing Strehl Ratios in Arbitrary Power Law Turbulence Spectra when $\beta L$ is such that the Power in a Finite Bandwidth is Constant*

In this comparison $\beta L$ is chosen such that the power in a finite bandwidth is constant. $\beta L$ is found using the following relation,

$$\int_{\kappa_1}^{\kappa_2} \mathrm{d}\kappa a(\alpha)\beta L\kappa^{-\alpha} - \int_{\kappa_1}^{\kappa_2} \mathrm{d}\kappa a(11/3)C_n^2 L\kappa^{-11/3} = 0. \tag{4.40}$$

The optimal way to accomplish this comparison would be to compute the total power in the spectrum instead of the power in a finite bandwidth. However, this is impossible for power law turbulence spectra since the total power is infinite. Figure (4.5) is a plot of Strehl ratio vs. power law for a 1 m diameter, circular source

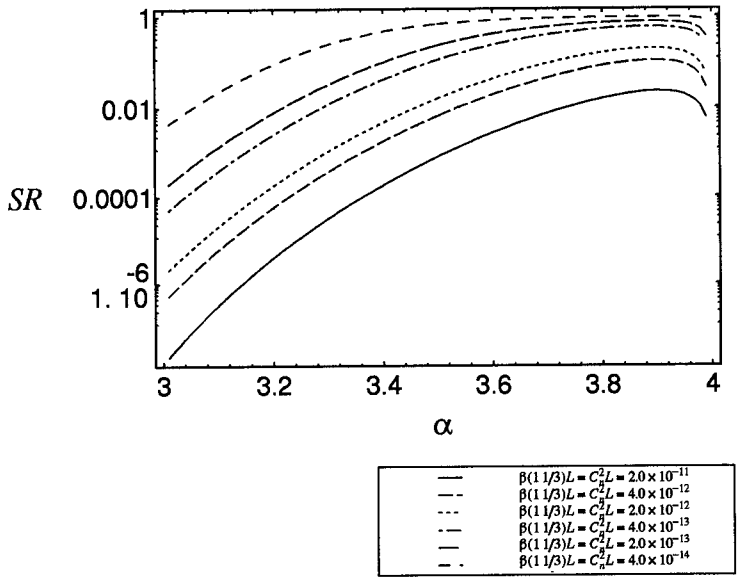


Figure 4.5 The Strehl ratio as a funtion of $\alpha$. $\beta L$ is chosen such that Eq. (4.40) is satisfied for the values of $C_n^2 L$ specified in the legend. The source aperture diameter $D$ is 1.0 m. The wavelength is 1.3 microns.

aperture. The bandwidth in which the spectral power is constrained to be equal is $.001 \leq \kappa \leq 100$. One can see a similar effect on $\beta L$ as in the previous section. In Figure (4.5) the constraint forces $\beta L$ to be large when $\alpha = 3$, thus $\rho_o$ and Strehl ratio are small. As the power law increases, the constraint forces $\beta L$ to become smaller until the effect of pure tilt again dominates when $\alpha \rightarrow 4$.

### *4.7 Comparing Strehl Ratios in Arbitrary Power Law Turbulence Spectra when $\beta L$ is such that the Piston-Removed Wave Variance is Constant*

The last basis used to compare the Strehl ratios as $\alpha$ varies, is to choose $\beta L$ such that the turbulence power spectra produce equal piston-removed wave variance.

The wave variance is defined as

$$\sigma_w^2 = \sigma_\chi^2 + \sigma_\phi^2, \tag{4.41}$$

where $\sigma_\chi^2$ is the log amplitude variance and $\sigma_\phi^2$ is the phase variance. Due to the infinite power in a general power law spectrum, the phase variance is infinite. Thus, Eq. (4.41) is infinite. However, if the piston component of the abberations to the optical wave is excluded, the phase variance is finite and the wave variance is calculable via Mellin transform techniques. Thus we are interested in the quantity

$$\sigma_{w_{-p}}^2 = \sigma_{\chi_{-p}}^2 + \sigma_{\phi_{-p}}^2, \tag{4.42}$$

where $-p$ indicates the removal of the piston component.

*4.7.1 Derivation of the piston-removed wave variance.* The spherical wave correlation functions for the scintillation and phase are rewritten from Eqs. (2.59 and 2.60):

$$B_\chi(\rho) = 4\pi^2 k^2 \int_0^L \mathrm{d}z \int_0^\infty \mathrm{d}\kappa\kappa J_0\left(\frac{\kappa\rho z}{L}\right) \sin^2\left[\frac{\kappa^2 z(L-z)}{2\kappa L}\right] \Phi_n(\kappa, z) \tag{4.43}$$

and

$$B_\phi(\rho) = 4\pi^2 k^2 \int_0^L \mathrm{d}z \int_0^\infty \mathrm{d}\kappa\kappa J_0\left(\frac{\kappa\rho z}{L}\right) \cos^2\left[\frac{\kappa^2 z(L-z)}{2\kappa L}\right] \Phi_n(\kappa, z). \tag{4.44}$$

Since $B_{\chi,\phi}(0) = \sigma_{\chi,\phi}^2$ and $\cos^2(x) + \sin^2(x) = 1$ the wave variance is

$$\sigma_w^2 = 4\pi^2 k^2 \int_0^L dz \int_0^\infty \mathrm{d}\kappa\kappa\Phi_n(\kappa, z). \tag{4.45}$$

Equation (4.45) is valid for both plane and spherical waves. Following the approach of Sasiela [23] and Noll [20], we can remove the effects of any Zernike mode by

introducing a filter function which removes the effects of that mode. The plane wave piston removed filter function is

$$F(\kappa, z) = 1 - 4\left[\frac{J_1(\kappa D/2)}{\kappa D/2}\right]^2. \tag{4.46}$$

Multiplying the integrand of Eq. (4.46) by the filter function gives

$$\sigma^2_{w_{-p}} = 4\pi^2 k^2 \int_0^L \mathrm{d}z \int_0^\infty \mathrm{d}\kappa \kappa \Phi_n(\kappa, z) \left\{1 - 4\left[\frac{J_1(\kappa D/2)}{\kappa D/2}\right]^2\right\}. \tag{4.47}$$

Substituting the turbulence power spectrum (Eq. (2.56)) into Eq. (4.47) yields

$$\sigma^2_{w_{-p}} = 4\pi^2 k^2 a(\alpha) \int_0^L dz \beta(z) \int_0^\infty \mathrm{d}\kappa \kappa^{1-\alpha} \left\{1 - 4\left[\frac{J_1(\kappa D/2)}{\kappa D/2}\right]^2\right\}. \tag{4.48}$$

Making the change of variables

$$\begin{aligned} x &= \frac{\kappa D}{2} \quad \mathrm{d}x = \frac{\mathrm{d}\kappa D}{2} \\ \kappa &= \frac{2x}{D} \quad \mathrm{d}\kappa = \frac{2\mathrm{d}x}{D}, \end{aligned} \tag{4.49}$$

yields

$$\sigma^2_{w_{-p}} = 4\pi^2 k^2 a(\alpha) \int_0^L dz \beta(z) \int_0^\infty \frac{2\mathrm{d}x}{D} (\frac{2x}{D})^{1-\alpha} \left[1 - 4x^{-2} J_1(x)^2\right]. \tag{4.50}$$

If we let $s = 2 - \alpha$, and multiply by $-1$, Eq. (4.50) becomes

$$\sigma^2_{w_{-p}} = -4\pi^2 k^2 a(\alpha) 2^s D^{-s} \int_0^L dz \beta(z) \int_0^\infty x^{s-1} \left\{4x^{-2} J_1(x)^2 - 1\right]. \tag{4.51}$$

Equation (4.51) is now in the form of a Mellin transform. From the tables in Sasiela [22],

$$M[x^a h(x)] \quad \rightarrow \quad H(s + a)$$

$$M[J_\nu^2(x)] \rightarrow \frac{1}{2\sqrt{\pi}}\Gamma\begin{bmatrix} s/2+\nu & 1/2-s/2 \\ \nu+1-s/2 & 1-s/2 \end{bmatrix} \quad -2\nu < \Re(s) < 1$$

$$M[1] \rightarrow \lim_{\epsilon\to 0}\left\{\frac{1}{s+\epsilon} - \frac{1}{s-\epsilon}\right\} \quad -\epsilon < \Re(s) < \epsilon. \tag{4.52}$$

Applying the transforms in Eq. (4.52) to Eq. (4.51) yields

$$\sigma^2_{w_{-p}} = -4\pi^2k^2a(\alpha)2^sD^{-s}\frac{2}{\sqrt{\pi}}\int_0^L dz\beta(z)$$
$$\times \lim_{\epsilon\to 0}\left\{\Gamma\begin{bmatrix} \frac{s-2}{2}+1 & 1/2-\frac{s-2}{2} \\ 2-\frac{s-2}{2} & 1-\frac{s-2}{2} \end{bmatrix} - \frac{1}{s+\epsilon} + \frac{1}{s-\epsilon}\right\} \quad -\epsilon < \Re(s) < \epsilon. \tag{4.53}$$

In the limit as $\epsilon \rightarrow 0$ the poles at $s = 0$ and $s = -\epsilon$ cancel and the path of the integration in the complex plane moves to the left one pole. Thus, Eq. (4.53) becomes

$$\sigma^2_{w_{-p}} = -4\pi^2k^2a(\alpha)\frac{2^{s+1}D^{-s}}{\sqrt{\pi}}\Gamma\begin{bmatrix} \frac{s}{2} & \frac{3-s}{2} \\ \frac{6-s}{2} & \frac{4-s}{2} \end{bmatrix} \quad -2 < \Re(s) < 0. \tag{4.54}$$

Since $s = 2 - \alpha$ the piston removed wave variance is

$$\sigma^2_{w_{-p}} = -4\pi^2k^2a(\alpha)\int_0^L \beta(z)dz\left\{\frac{2^{3-\alpha}D^{\alpha-2}}{\sqrt{\pi}}\Gamma\begin{bmatrix} \frac{2-\alpha}{2} & \frac{1-\alpha}{2} \\ \frac{4+\alpha}{2} & \frac{2+\alpha}{2} \end{bmatrix}\right\} \quad 2 < \alpha < 4. \tag{4.55}$$

If $\beta(z)$ is constant over the path $L$, the piston removed wave variance is

$$\sigma^2_{w_{-p}} = -2^{5-\alpha}\pi^{3/2}k^2a(\alpha)\beta L\Gamma\begin{bmatrix} \frac{2-\alpha}{2} & \frac{1-\alpha}{2} \\ \frac{4+\alpha}{2} & \frac{2+\alpha}{2} \end{bmatrix}D^{\alpha-2} \quad 2 < \alpha < 4. \tag{4.56}$$

*4.7.2 Comparing Strehl ratios in arbitrary power law turbulence spectra when $\beta L$ is such that the piston removed wave variance is constant.* In this comparison $\beta L$ is chosen such that the piston removed wave variance is constant. $\beta L$ is found

using the following relation,

$$\sigma^2_{w_{-p}}(a(\alpha),\beta,L,\alpha) - \sigma^2_{w_{-p}}(a(11/3),C_n^2,L,11/3) = 0. \tag{4.57}$$

Solving Eq. (4.57) for $\beta L$ yields

$$\beta L = -2^{-(11/3+\alpha)}\frac{a(11/3)}{a(\alpha)}C_n^2 L D^{11/3-\alpha}\Gamma\begin{bmatrix} -\frac{5}{6} & -\frac{8}{6} & \frac{4+\alpha}{2} & \frac{2+\alpha}{2} \\ \frac{33}{6} & \frac{16}{6} & \frac{2-\alpha}{2} & \frac{1-\alpha}{2} \end{bmatrix} \qquad 2 < \alpha < 4 \tag{4.58}$$

Figure (4.6) is a plot of the Strehl ratio as a function of the power law $\alpha$ for a 1 m diameter, circular source aperture. The wavelength is 1.3 microns. One can see in

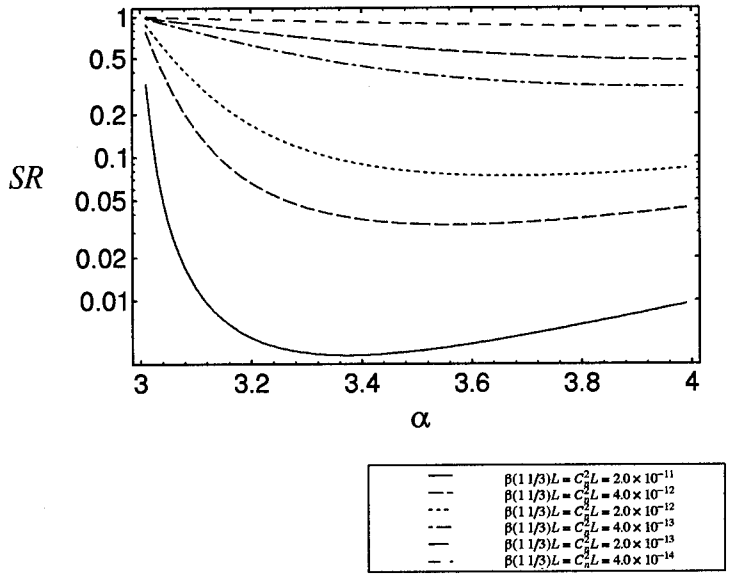


Figure 4.6 The Strehl ratio as a function of the power law. $\beta L$ is chosen such that Eq. (4.58) is satisfied for the values of $C_n^2 L$ specified in the legend. The source aperture diameter $D$ is 1.0 m. The wavelength is 1.3 microns.

Fig. (4.58) that the constraint on $\beta L$ now behaves differently depending the strength of the turbulence. If the turbulence is weak, changing the power law has little effect under this constraint. If the turbulence is strong $\beta L$ can be quite small at $\alpha = 3$, thus Strehl ratio can approach 1.

# V. *Contributions of the Log Amplitude and Phase Structure Functions*

Adaptive optical systems systems can only compensate for phase fluctuations in an optical beam. Therefore, if a distorted beam contains more phase fluctuations and less log amplitude fluctuations, an adaptive optic compensation system can be expected to perform a high percentage of correction.

In the previous chapters we were concerned with the wave structure function $D_w(\rho)$. It was shown in Chapter 2 that the wave structure function is actually the sum of the log amplitude and phase structure functions. The goal of this chapter is to determine the conditions under which either phase or amplitude perturbations to the optical beam dominate, as the power law $\alpha$ is varied from $3 < \alpha < 4$. This will be done by plotting the relative contributions of the log amplitude $D_\chi(\rho)$ and phase $D_\phi(\rho)$ structure functions to the wave structure function $D_w(\rho)$.

Rewriting Eqs. (2.61) and (2.62) gives

$$D_w(\rho) = D_\chi(\rho) + D_\phi(\rho) \tag{5.1}$$

and

$$D_\chi(\rho) = 2[B_\chi(0) - B_\chi(\rho)] \tag{5.2}$$

and

$$D_\phi(\rho) = 2[B_\phi(0) - B_\phi(\rho)]. \tag{5.3}$$

The log amplitude and phase correlation funtions are rewritten from Eqs. (2.59 and 2.60)

$$B_\chi(\rho) = 4\pi^2 k^2 \int_0^L \mathrm{d}z \int_0^\infty \mathrm{d}\kappa\, \kappa J_0\left(\frac{\kappa\rho z}{L}\right) \sin^2\left[\frac{\kappa^2 z(L-z)}{2kL}\right] \Phi_n(\kappa, z) \tag{5.4}$$

and

$$B_\phi(\rho) = 4\pi^2 k^2 \int_0^L \mathrm{d}z \int_0^\infty \mathrm{d}\kappa\, \kappa J_0\left(\frac{\kappa\rho z}{L}\right) \cos^2\left[\frac{\kappa^2 z(L-z)}{2kL}\right] \Phi_n(\kappa, z), \tag{5.5}$$

where $J_0$ is a Bessel function of the first kind, order 0, $k$ is the optical wavenumber, $\rho$ is the geometrical separation between points in the source plane, and $L$ is the length of the optical path. By substituting Eqs. (5.4 and 5.5) into Eq. (5.2) we get

$$D_\chi(\rho) = 8\pi^2 k^2 \int_0^L \mathrm{d}z \int_0^\infty \mathrm{d}\kappa\, \kappa \left[1 - J_0(\frac{\kappa\rho z}{L})\right] \sin^2\left(\frac{\kappa^2 z(L-z)}{2kz}\right) \Phi_n(\kappa, \alpha, z) \tag{5.6}$$

and

$$D_\phi(\rho) = 8\pi^2 k^2 \int_0^L \mathrm{d}z \int_0^\infty \mathrm{d}\kappa\, \kappa \left[1 - J_0(\frac{\kappa\rho z}{L})\right] \cos^2\left(\frac{\kappa^2 z(L-z)}{2kz}\right) \Phi_n(\kappa, \alpha, z). \tag{5.7}$$

The arbitrary power law turbulence spectrum from Eq. (2.56) is

$$\Phi_n(\kappa, \alpha, z) = a(\alpha)\beta(z)\kappa^{-\alpha}. \tag{5.8}$$

Substituting Eq. (5.8) into Eqs. (5.6 and 5.7) yields

$$D_\chi(\rho) = 8\pi^2 k^2 a(\alpha) \int_0^L \mathrm{d}z \beta(z) \int_0^\infty \mathrm{d}\kappa\, \kappa^{1-\alpha} \left[1 - J_0(\frac{\kappa\rho z}{L})\right] \sin^2\left(\frac{\kappa^2 z(L-z)}{2kz}\right) \tag{5.9}$$

and

$$D_\phi(\rho) = 8\pi^2 k^2 a(\alpha) \int_0^L \mathrm{d}z \beta(z) \int_0^\infty \mathrm{d}\kappa\, \kappa^{1-\alpha} \left[1 - J_0(\frac{\kappa\rho z}{L})\right] \cos^2\left(\frac{\kappa^2 z(L-z)}{2kz}\right). \tag{5.10}$$

To derive some general conclusions about the behavior of Eqs. (5.9) and (5.10) consider the change of variables

$$z' = \frac{z}{L} \quad \mathrm{d}z' = \frac{\mathrm{d}_z}{L}$$
$$z = z'L \quad \mathrm{d}z = \mathrm{d}z'L,$$

thus Eqs. (5.9) and (5.10) become

$$D_\chi(\rho) = 8\pi^2 k^2 a(\alpha) \int_0^1 \mathrm{d}z' \beta(z'L) \int_0^\infty \mathrm{d}\kappa\, \kappa^{1-\alpha} \left[1 - J_0(\kappa\rho z')\right] \sin^2\left(\frac{\kappa^2 z'(1-z')L}{2k}\right) \quad (5.11)$$

and

$$D_\phi(\rho) = 8\pi^2 k^2 a(\alpha) \int_0^1 \mathrm{d}z' \beta(z'L) \int_0^\infty \mathrm{d}\kappa\, \kappa^{1-\alpha} \left[1 - J_0(\kappa\rho z')\right] \cos^2\left(\frac{\kappa^2 z'(1-z')L}{2k}\right). \quad (5.12)$$

One can normalize the wavelength and path length dependencies by defining the parameter Fresnel ratio ($FR$) which is the ratio of the separation of points in the source plane divided by the Fresnel number scaled by $4\pi$

$$FR = \frac{4\pi\rho^2}{\lambda L} = \frac{4\pi\rho^2}{FN^2}. \quad (5.13)$$

Substituting Eq. (5.13) into Eqs. (5.11) and (5.12) yields

$$D_\chi(\rho) = 8\pi^2 k^2 a(\alpha) \int_0^1 \mathrm{d}z' \beta(z'L) \int_0^\infty \mathrm{d}\kappa\, \kappa^{1-\alpha} \left[1 - J_0(\kappa\rho z')\right] \sin^2\left(\frac{(\kappa\rho)^2 z'(1-z')}{FR}\right) \quad (5.14)$$

and

$$D_\phi(\rho) = 8\pi^2 k^2 a(\alpha)$$
$$\int_0^1 \mathrm{d}z' \beta(z'L) \int_0^\infty \mathrm{d}\kappa\, \kappa^{1-\alpha} \left[1 - J_0(\kappa\rho z')\right] \cos^2\left(\frac{(\kappa\rho)^2 z'(1-z')}{FR}\right). \quad (5.15)$$

The problem is now reduced to a double integration over the turbulence frequency variable $\kappa$ and the normalized path $z'$. Eqs. (5.14) and (5.15) contain a product of functions in $\kappa$ which yield an integrand that is highly oscillatory in the $\kappa, z'$ plane and does not decay rapidly. This makes numerical integration of Eqs. (5.14) and (5.15) over both $\kappa$ and $z'$ quite difficult. Luckily, both integrals can be evaluated over $\kappa$ in closed form using advanced Mellin transform techniques according to the following procedure:

1. Use the Mellin convolution theorem to transform the real integral into a Mellin-Barnes contour integral in complex plane. Consider the integral

$$h(x) = \int_0^\infty y^{-1} h_o(y) h_1(x/y) \mathrm{d}y. \quad (5.16)$$

Take the Mellin transform of h(x)

$$\mathcal{M}(h(x)) = \int_0^\infty \int_0^\infty y^{-1} h_o(y) h_1(x/y) x^{s-1} \mathrm{d}y \mathrm{d}x. \quad (5.17)$$

By making the change of variables $w = x/y$, thus $x = wy$ and $\mathrm{d}x = y\mathrm{d}w$ and interchanging the order of integration Eq. (5.17) becomes

$$\mathcal{M}(h(x)) = \int_0^\infty y^{-1} h_o(y) \mathrm{d}y \int_0^\infty (wy)^{s-1} h_1(w) y \mathrm{d}w. \quad (5.18)$$

Simplifying Eq. (5.18) yields an integral of the Mellin transforms of $h_o$ and $h_1$

$$\mathcal{M}(h(x)) = \int_0^\infty y^{s-1} h_o(y) \mathrm{d}y \int_0^\infty (w)^{s-1} h_1(w) \mathrm{d}w = H_o(s) H_1(s). \quad (5.19)$$

The inverse Mellin transform is now the contour integral

$$h(x) = \frac{1}{2\pi j}\int_c H_o(s)H_1(s)x^{-s}\mathrm{d}s, \tag{5.20}$$

where $H_o(s)$ and $H_1(s)$ are the individual Mellin transforms of $h_o(y)$ and $h_1(x/y)$. Since the Mellin transforms of $h_o(y)$ and $h_1(x/y)$ in Eq. (5.20) can be expressed as ratios of gamma functions, the original integral $h(x)$ (Eq. 5.16) can be expressed as a Mellin-Barnes integral of the following form:

$$h(x) = \frac{1}{2\pi j}\int_c \mathrm{d}s x^{-s}\frac{\Pi_{i=1}^{A}\Gamma[a_i+\alpha_i s]\Pi_{j=1}^{B}\Gamma[b_j-\beta_j s]}{\Pi_{k=1}^{C}\Gamma[c_k+\gamma_k s]\Pi_{m=1}^{D}\Gamma[d_m+\delta_m s]}. \tag{5.21}$$

2. Close the path of the contour integral at infinity, subject to the conditions specified in [22] and perform the contour integration using Cauchy's residue theorem. Application of the residue theorem yields an infinite sum of the residues at the poles of the gamma functions in Eq. (5.21)

$$h(x) = \sum_n x^{-s_n} Res(s_n). \tag{5.22}$$

The poles occur only when $s = -(n+a_i)/\alpha_i$ or $s = -(n+b_j)/\beta_j$.

3. Use the definition of a generalized hypergeometric function to convert the infinite sum found in Step 2 into a sum of generalized hypergeometric functions. The definition of a generalized hypergeometric function is given by [22]

$${}_pF_q(a,b,z) = \sum_{k=0}^{\infty}\frac{z^k}{k!}\frac{(a_1)_k(a_2)_k\ldots(a_p)_k}{(b_1)_k(b_2)_k\ldots(b_1)_k}, \tag{5.23}$$

where $(a) = a_1, a_2, \ldots, a_p$, $(b) = b_1, b_2, \ldots, b_q$ and $(a)_k$ is the Pochhammer symbol defined as

$$(a)_k = \frac{\Gamma[a+k]}{\Gamma[a]}. \tag{5.24}$$

Although the procedure outlined above seems quite difficult to the uninitiated, the method reduces to a series of straightforward and logical, but somewhat tedious steps. The details are shown in Sasiela [22].

Fortunately in this case there is a short cut, the $\kappa$ integration in Eqs. (5.14) and (5.15) can be accomplished using Mathematica's [29] symbolic integration routines. Unfortunately Mathematica does not always produce symbolic output in the most convienient form, either for physical interpretation or numerical condition. In the case of Eqs. (5.14 and 5.15) the Mathematica solution is sufficiently well behaved to allow numerical integration over $z'$ for the ranges of the parameters of interest ($FR$ and $\alpha$). The results of the $\kappa$ space integrations performed using Mathematica are contained in unreduced form in Appendix A.

Once the integration over $\kappa$ is performed, the sum of generalized hypergeometric functions created in Step 3 can be numerically integrated over the normalized path to get the log amplitude and phase structure functions.

Since we are concerned with the relative contributions of the log amplitude and phase structure functions to the wave structure function, we can examine the ratios $D_\chi(\rho)/D_w(\rho)$ and $D_\phi(\rho)/D_w(\rho)$ which are given by

$$\frac{D_\chi(\rho)}{D_w(\rho)} = \frac{\int_0^1 \mathrm{d}z'\beta(z'L)\int_0^\infty \mathrm{d}\kappa\,\kappa^{1-\alpha}\left[1-J_0(\kappa\rho z')\right]\sin^2\left(\frac{(\kappa\rho)^2 z'(1-z')}{FR}\right)}{\int_0^1 \mathrm{d}z'\beta(z'L)\int_0^\infty \mathrm{d}\kappa\,\kappa^{1-\alpha}\left[1-J_0(\kappa\rho z')\right]} \tag{5.25}$$

and

$$\frac{D_\phi(\rho)}{D_w(\rho)} = \frac{\int_0^1 \mathrm{d}z'\beta(z'L)\int_0^\infty \mathrm{d}\kappa\,\kappa^{1-\alpha}\left[1-J_0(\kappa\rho z')\right]\cos^2\left(\frac{(\kappa\rho)^2 z'(1-z')}{FR}\right)}{\int_0^1 \mathrm{d}z'\beta(z'L)\int_0^\infty \mathrm{d}\kappa\,\kappa^{1-\alpha}\left[1-J_0(\kappa\rho z')\right]}. \tag{5.26}$$

Close examination of the equations for $D_\chi(\rho)$ and $D_\phi(\rho)$ in Appendix A shows both contain a dependence on $\rho^{\alpha-2}$. The wave structure function, Eq. (2.70) derived in Chapter 2, also contains a $\rho^{\alpha-2}$ dependence. Therefore ratios $D_\chi(\rho)/D_w(\rho)$ and $D_\phi(\rho)/D_w(\rho)$ do not depend on $\rho$ directly. However, the ratios $D_\chi(\rho)/D_w(\rho)$ and

$D_\phi(\rho)/D_w(\rho)$ do depend on $\rho$ indirectly through the definition of Fresnel ratio in Eq. (5.13).

Figure (5.1) contains a plot of the ratios $D_\chi(\rho)$ and $D_\phi(\rho)$ as a function of the power law $\alpha$ for various Fresnel ratio's $FR$. The upper family of curves are the phase contributions $D_\phi(\rho)$ to the wave structure function $D_w(\rho)$ and the lower family of curves are the log amplitude contributions to the wave structure function $D_w(\rho)$. The sum of the log amplitude and phase contributions equals 1. Two key

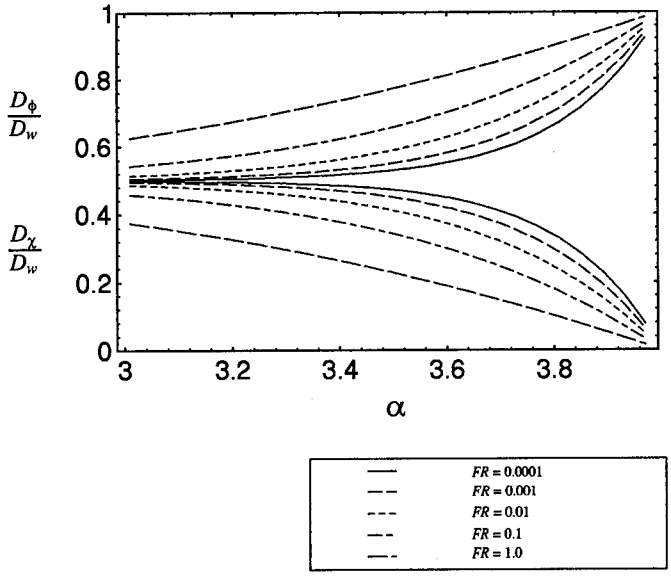


Figure 5.1 The relative contributions of the log amplitude and phase structure functions to the wave structure funtion as a function of the power law $\alpha$. The Fresnel ratio $FR$ is fixed at the value specified in the legend.

observations can be made from this plot. Phase perturbations increase as Fresnel ratio increases. This is consistent with the definition of Fresnel ratio. For a fixed separation $\rho$ in the source plane, the phase effects get large as the Fresnel *number* decreases. In other words phase effects increase when the optical path is short. The

second and most important observation is that phase effects dominate as the power law increases to $\alpha = 4$. This is consistent with the work of Heidbreder [12] who showed that a wave structure function which had a $\rho^2$ dependence corresponded to a pure random tilt in the aperture of an incoherent imaging system.

# *VI. Results, Conclusions, and Recommendations*

This chapter summarizes the major results of this research. Following the summary, the implications for adaptive optical beamforming systems are discussed and recommendations for future research are made.

## *6.1 Summmary of Results*

In Chapter 2, Section 2.2, the fundamental relationship between the index structure function and the index power spectrum were examined. Assuming the turbulence is isotropic and the index structure function obeys an arbitrary power law

$$D_n(\rho) = \beta(z)\rho^{\alpha-3}, \tag{6.1}$$

the corresponding index power spectrum is

$$\Phi_n(\kappa) = a(\alpha)\beta(z)\kappa^{-\alpha}, \tag{6.2}$$

where the function $a(\alpha)$ maintains consistency between the index structure function and the index power spectrum and is given by

$$a(\alpha) \equiv 2^{\alpha-6}(\alpha^2 - 5\alpha + 6)\pi^{-3/2}\frac{\Gamma\left[\frac{\alpha-2}{2}\right]}{\Gamma\left[\frac{5-\alpha}{2}\right]} \quad 3 < \alpha < 5. \tag{6.3}$$

Inner and outer scale effects were neglected.

In Sections 2.3 and 2.4 the wave structure function was derived using the log amplitude and phase correlation functions which can be derived from the method of small perturbations. The wave structure function is given by

$$D_w(\rho) = c_1\left(\frac{\rho}{\rho_o}\right)^{\alpha-2}, \tag{6.4}$$

where $c_1$ is given by

$$c_1 = 2\left(\frac{8}{\alpha-2}\Gamma\left[\frac{2}{\alpha-2}\right]\right)^{\frac{\alpha-2}{2}} \tag{6.5}$$

and a new generalized definition for the coherence diameter is

$$\rho_o = \left\{\frac{c_1(\alpha-1)\Gamma\left[\frac{\alpha}{2}\right]}{-(2)^{4-\alpha}\pi^2 k^2 a(\alpha) L^{2-\alpha}\Gamma\left[\frac{2-\alpha}{2}\right]\int_0^L \beta(z) z^{\alpha-2} \mathrm{d}z}\right\}^{\frac{1}{\alpha-2}} \quad 3<\alpha<4. \tag{6.6}$$

The important conclusions to draw from Sections 2.3 and 2.4 are, if inner and outer scale effects are neglected, only power laws from $3 < \alpha < 4$ are allowed to exist. The physical interpretations for the mathematical results are:

1. When the power law $\alpha \to 3$, the index structure function, Eq. (6.1), has no dependence on $\rho$, therefore no turbulence exists.
2. When the power law $\alpha \to 4$, the wave structure function, Eq. (6.4), has a $\rho^2$ dependence and the resulting abberation to the optical wave is a random tilt in the source aperture which causes the beam to wander, thereby dramatically increasing the long exposure spot size.

In Section 2.5 the variance of the log amplitude fluctuations was found to be

$$\sigma_\chi^2 = \frac{4c_1\pi^{\frac{3-\alpha}{2}}}{\alpha}\left(\frac{FN}{\rho_o}\right)^{\alpha-2}\Gamma\left[\begin{array}{cc}\frac{2-\alpha}{4} & \frac{\alpha}{2} \\ \frac{\alpha}{4} & \frac{2-\alpha}{2}\end{array}\right], \tag{6.7}$$

where $FN$ is the Fresnel number defined as

$$FN = \sqrt{\lambda L}. \tag{6.8}$$

The log amplitude variance is a maximum as $\alpha \to 3$. The value of the maximum log amplitude variance is determined by the ratio of the Fresnel number to the coherence diameter ($FN/\rho_o$). The log amplitude variance decreases greatly as $\alpha \to 4$ and phase effects dominate.

In Chapter 3, the mutual coherence function of an arbitrary wave propagating through turbulence which obeys an arbitrary power spectrum was derived. The result is a 4-dimensional integral of the form

$$\begin{aligned} &MCF(x_1, y_1, x_2, y_2) = \\ &\quad (\frac{k}{2\pi z})^2 \psi \iiiint H(x_1, y_1, \xi_1, \eta_1, x_2, y_2, \xi_2, \eta_2, z) \\ &\quad \times \exp\left[\frac{jk}{2z}((\xi_1^2 + \eta_1^2) - (\xi_2^2 + \eta_2^2) + 2x_2\xi_2 - 2x_1\xi_1 + 2y_2\eta_2 - 2y_1\eta_1)\right] \\ &\quad \times U_A(\xi_1, \eta_1) U_A^*(\xi_2, \eta_2) \mathrm{d}\xi_1 \mathrm{d}\eta_1 \mathrm{d}\xi_2 \mathrm{d}\eta_2, \end{aligned} \tag{6.9}$$

where $H(x_1, y_1, \xi_1, \eta_1, x_2, y_2, \xi_2, \eta_2, z)$ is the second moment of the Greens function for propagation of a spherical wave in a turbulent medium. $H(x_1, y_1, \xi_1, \eta_1, x_2, y_2, \xi_2, \eta_2, z)$ is shown in [17] to be

$$H(x_1, y_1, \xi_1, \eta_1, x_2, y_2, \xi_2, \eta_2, z) = \exp\left[-\frac{1}{2} D_w(\rho)\right]. \tag{6.10}$$

From the general form of Eq. (6.9) many parameters of interest can be calculated, including intensity profiles and Strehl ratios for arbitrary apertures.

The Strehl ratio of a constant amplitude beam is derived in Chapter 4. The MCF derived in Chapter 3 was reduced to a single numerical integral of the form

$$\mathcal{SR} = \frac{32}{\pi} \int_0^1 \frac{1}{2}(\cos^{-1}(u) - u\sqrt{1-u^2}) \exp\left[-\frac{1}{2} c_1 \left(\frac{D}{\rho_o} u\right)^{\alpha-2}\right] u \mathrm{d}u. \tag{6.11}$$

Several comparisons of the Strehl ratio as a function of the power law $\alpha$ were made under various constraints. It was necessary to use a variety of constraints to compare the Strehl ratio at power law $\alpha_1$ to Strehl ratio at another power law $\alpha_2$ because changing $\alpha$ changes the total power in the turbulence spectrum, therefore biasing the results one way or another. In general, the resulting trends of the Strehl ratio depend on the constraint placed on the integrated turbulence strength $\beta L$ as the

power law $\alpha$ was varied. The consistent trend noticed in the behavior of the Strehl ratio was that the Strehl ratio approached zero as $\alpha \rightarrow 4$, this behavior is consistent with the physical model of a pure tilt aberration in the source aperture.

In Section 4.2 the asymptotic behavior of Fried's $\mathcal{R}/\mathcal{R}_{max}$ resolution metric was examined for a general power law. The design of this metric is such that when the power law $\alpha$ is varied from $3 < \alpha < 4$, it is possible to define the generalized coherence diameter $\rho_o$ and the constant $c_1$, such that the interpretation of $\rho_o$ is the same as Fried's coherence diameter for Kolmogorov turbulence, $r_o$.

Finally, in Chapter 5 the relative contributions of the log amplitude and phase structure functions to the wave structure functions were calculated. This analysis showed conclusively that

1. As the power law $\alpha \rightarrow 3$ the relative contributions of the log amplitude and phase fluctuations are soley controlled by the Fresnel ratio of the system.
2. As the power law $\alpha \rightarrow 4$ phase effects dominate the wave structure function regardless of Fresnel ratio.

It is postulated from the results of Chapters 4 and 5 that if the perturbations of the wavefront in the source plane is decomposed into a series of Zernike polynomials, the energy in the series shifts toward the low order modes when the power law $\alpha$ increases towards 4.

### *6.2 Implications for Adaptive Optical Beamforming Systems*

An adaptive optical beamforming system corrects for atmospheric effects by predistorting the phase of the wavefront to be transmitted with the conjugate of the phase perturbations induced in the atmosphere. Thus, atmospheric conditions which yield only phase perturbations are more conducive to the operation of adaptive optical systems. This means turbulence power spectra which have power laws approaching 4 are more conducive to the operation of adaptive optical systems. For

equal turbulence strength, the ABL system can expect better performance in turbulence whose power law tends toward $\alpha = 4$. The converse is also true, regardless of the Fresnel ratio of the system, the ABL system can expect worse performance as $\alpha \rightarrow 3$.

Additionally, if the limit on the method of small perturbations ($\sigma_\chi^2 \leq 0.3 - 0.5$) is assumed to hold regardless of the power law, the method of small perturbations can be used at longer path lengths and greater turbulence strengths than previously determined if $\alpha \rightarrow 4$.

### *6.3 Recommendations for Future Research*

In this section several extensions of this research are proposed.

1. Determine the frequency response of the ARGUS anemometer probes. This is the highest priority, because without an accurate calibration of the frequency response the ARGUS anemometer data is inconclusive. With the current data it is impossible to separate the effects of inner and outer scales of turbulence from the power law of the inertial subrange and from the probe response. Once the calibration has been accomplished, these effects are separable and one could determine the directions of further investigations into non-Kolmogorov propagation theory.
2. Perform a modal decomposition of the propagating wavefront using Zernike polynomials. By estimating the average energy associated with each polynomial in the series, the postulate in Section 6.2 can be proved or disproved.
3. The analysis presented in this thesis neglected the effects of an inner and outer scale. A generalized power spectrum incorporating the effects of an inner and outer scale can be defined as

$$\Phi_n(\kappa, \alpha, z) = a'(\alpha)\beta(z)(\kappa^2 + \kappa_o^2)^{-\alpha/2} \exp\left[\frac{\kappa^2}{\kappa_m^2}\right], \tag{6.12}$$

where $\kappa_m$ and $\kappa_o$ are the inner and outer scales, respectively. Note: $a'(\alpha)$ in Eq. (6.12) is not the $a(\alpha)$ defined in this thesis.

## *Appendix A. Integration of the Log Amplitude and Phase Structure Functions*

In Chapter 5, Mathematica was used to evaluate the following integrals. The integrals over the turbulence wavenumber $\kappa$ were evaluated in closed form. The integrals over the path $z'$ were evaluated numerically. Specifically, from Eqs. (5.14 and 5.15) we have

$$D_\chi(\rho) = 8\pi^2 k^2 a(\alpha) \times \int_0^1 \mathrm{d}z' \beta(z'L) \int_0^\infty \mathrm{d}\kappa\, \kappa^{1-\alpha} \left[1 - J_0(\kappa\rho z')\right] \sin^2\left(\frac{(\kappa\rho)^2 z'(1-z')}{FR}\right) \quad \text{(A.1)}$$

and

$$D_\phi(\rho) = 8\pi^2 k^2 a(\alpha) \times \int_0^1 \mathrm{d}z' \beta(z'L) \int_0^\infty \mathrm{d}\kappa\, \kappa^{1-\alpha} \left[1 - J_0(\kappa\rho z')\right] \cos^2\left(\frac{(\kappa\rho)^2 z'(1-z')}{FR}\right). \quad \text{(A.2)}$$

Integrating Eq. (A.1) symbolically over $\kappa$ gives

$$D_\chi(\rho) = 8\pi^2 k^2 a(\alpha) \int_0^1 \mathrm{d}z' \beta(z'L) \quad \text{(A.3)}$$

$$\frac{\frac{1}{4}^{\frac{\alpha}{2}}\, FR^2\, \pi \left(\rho^2\, z^2\right)^{\frac{\alpha}{2}}\, \csc(\frac{\alpha\,\pi}{4})\, {}_{\mathrm{p}}F_{\mathrm{q}}(\{1-\frac{\alpha}{4}, \frac{3}{2}-\frac{\alpha}{4}\}, \{1, \frac{3}{2}, \frac{3}{2}\}, \frac{-\left(\mathrm{FR}^2\, z^2\right)}{256\,(1-z)^2})}{128\, \frac{1}{256}^{\frac{\alpha}{4}}\, 2^{\frac{\alpha}{2}} \left(-1+\frac{\alpha}{4}\right) \rho^2\, (1-z)^2\, \frac{\mathrm{FR}^2\, z^2}{(1-z)^2}^{\frac{\alpha}{4}}\, \Gamma(-1+\frac{\alpha}{2})} -$$

$$\frac{\frac{1}{4}^{\frac{\alpha}{2}}\, \alpha\, FR^2\, \pi \left(\rho^2\, z^2\right)^{\frac{\alpha}{2}}\, \csc(\frac{\alpha\,\pi}{4})\, {}_{\mathrm{p}}F_{\mathrm{q}}(\{1-\frac{\alpha}{4}, \frac{3}{2}-\frac{\alpha}{4}\}, \{1, \frac{3}{2}, \frac{3}{2}\}, \frac{-\left(\mathrm{FR}^2\, z^2\right)}{256\,(1-z)^2})}{512\, \frac{1}{256}^{\frac{\alpha}{4}}\, 2^{\frac{\alpha}{2}} \left(-1+\frac{\alpha}{4}\right) \rho^2\, (1-z)^2\, \frac{\mathrm{FR}^2\, z^2}{(1-z)^2}^{\frac{\alpha}{4}}\, \Gamma(-1+\frac{\alpha}{2})} +$$

$$\frac{3\, \frac{1}{4}^{\frac{\alpha}{2}}\, \pi \left(\rho^2\, z^2\right)^{\frac{\alpha}{2}}\, \frac{\mathrm{FR}^2\, z^2}{(1-z)^2}^{\frac{3}{2}-\frac{\alpha}{4}}\, \sec(\frac{\alpha\,\pi}{4})}{128\, \frac{1}{256}^{\frac{\alpha}{4}}\, 2^{\frac{\alpha}{2}} \left(\frac{1}{2}-\frac{\alpha}{4}\right) \left(1-\frac{\alpha}{4}\right) \left(-\frac{3}{2}+\frac{\alpha}{4}\right) FR^2\, \rho^2\, z^4\, \Gamma(-2+\frac{\alpha}{2})} -$$

$$\frac{\frac{1}{4}^{\frac{\alpha}{2}}\, \alpha\, \pi \left(\rho^2\, z^2\right)^{\frac{\alpha}{2}}\, \frac{\mathrm{FR}^2\, z^2}{(1-z)^2}^{\frac{3}{2}-\frac{\alpha}{4}}\, \sec(\frac{\alpha\,\pi}{4})}{256\, \frac{1}{256}^{\frac{\alpha}{4}}\, 2^{\frac{\alpha}{2}} \left(\frac{1}{2}-\frac{\alpha}{4}\right) \left(1-\frac{\alpha}{4}\right) \left(-\frac{3}{2}+\frac{\alpha}{4}\right) FR^2\, \rho^2\, z^4\, \Gamma(-2+\frac{\alpha}{2})} -$$

$$\frac{3\, \frac{1}{4}^{\frac{\alpha}{2}}\, \pi \left(\rho^2\, z^2\right)^{\frac{\alpha}{2}}\, \frac{\mathrm{FR}^2\, z^2}{(1-z)^2}^{\frac{3}{2}-\frac{\alpha}{4}}\, \sec(\frac{\alpha\,\pi}{4})}{64\, \frac{1}{256}^{\frac{\alpha}{4}}\, 2^{\frac{\alpha}{2}} \left(\frac{1}{2}-\frac{\alpha}{4}\right) \left(1-\frac{\alpha}{4}\right) \left(-\frac{3}{2}+\frac{\alpha}{4}\right) FR^2\, \rho^2\, z^3\, \Gamma(-2+\frac{\alpha}{2})} +$$

$$\frac{\frac{1}{4}^{\frac{\alpha}{2}}\,\alpha\,\pi\left(\rho^2\,z^2\right)^{\frac{\alpha}{2}}\,\frac{\mathrm{FR}^2\,z^2}{(1-z)^2}^{\frac{3}{2}-\frac{\alpha}{4}}\,\sec(\frac{\alpha\,\pi}{4})}{128\,\frac{1}{256}^{\frac{\alpha}{4}}\,2^{\frac{\alpha}{2}}\left(\frac{1}{2}-\frac{\alpha}{4}\right)\left(1-\frac{\alpha}{4}\right)\left(-\frac{3}{2}+\frac{\alpha}{4}\right)FR^2\,\rho^2\,z^3\,\Gamma(-2+\frac{\alpha}{2})}+$$

$$\frac{3\,\frac{1}{4}^{\frac{\alpha}{2}}\,\pi\left(\rho^2\,z^2\right)^{\frac{\alpha}{2}}\,\frac{\mathrm{FR}^2\,z^2}{(1-z)^2}^{\frac{3}{2}-\frac{\alpha}{4}}\,\sec(\frac{\alpha\,\pi}{4})}{128\,\frac{1}{256}^{\frac{\alpha}{4}}\,2^{\frac{\alpha}{2}}\left(\frac{1}{2}-\frac{\alpha}{4}\right)\left(1-\frac{\alpha}{4}\right)\left(-\frac{3}{2}+\frac{\alpha}{4}\right)FR^2\,\rho^2\,z^2\,\Gamma(-2+\frac{\alpha}{2})}-$$

$$\frac{\frac{1}{4}^{\frac{\alpha}{2}}\,\alpha\,\pi\left(\rho^2\,z^2\right)^{\frac{\alpha}{2}}\,\frac{\mathrm{FR}^2\,z^2}{(1-z)^2}^{\frac{3}{2}-\frac{\alpha}{4}}\,\sec(\frac{\alpha\,\pi}{4})}{256\,\frac{1}{256}^{\frac{\alpha}{4}}\,2^{\frac{\alpha}{2}}\left(\frac{1}{2}-\frac{\alpha}{4}\right)\left(1-\frac{\alpha}{4}\right)\left(-\frac{3}{2}+\frac{\alpha}{4}\right)FR^2\,\rho^2\,z^2\,\Gamma(-2+\frac{\alpha}{2})}+$$

$$\frac{\frac{1}{4}^{\frac{\alpha}{2}}\,\sqrt{\pi}\left(\rho^2\,z^2\right)^{\frac{\alpha}{2}}\,\Gamma(1-\frac{\alpha}{4})\,\sec(\frac{\alpha\,\pi}{4})}{2\,2^{\frac{\alpha}{2}}\left(-\frac{1}{2}+\frac{\alpha}{4}\right)\rho^2\,z^2\,\Gamma(\frac{1}{2}+\frac{\alpha}{4})\,\Gamma(\frac{\alpha}{2})}-$$

$$\frac{\frac{1}{4}^{\frac{\alpha}{2}}\,\alpha\,\sqrt{\pi}\left(\rho^2\,z^2\right)^{\frac{\alpha}{2}}\,\Gamma(1-\frac{\alpha}{4})\,\sec(\frac{\alpha\,\pi}{4})}{4\,2^{\frac{\alpha}{2}}\left(-\frac{1}{2}+\frac{\alpha}{4}\right)\rho^2\,z^2\,\Gamma(\frac{1}{2}+\frac{\alpha}{4})\,\Gamma(\frac{\alpha}{2})}-$$

$$\frac{3\,\frac{1}{4}^{\frac{\alpha}{2}}\,\pi\left(\rho^2\,z^2\right)^{\frac{\alpha}{2}}\,\frac{\mathrm{FR}^2\,z^2}{(1-z)^2}^{\frac{3}{2}-\frac{\alpha}{4}}\,{}_pF_q(\{\frac{1}{2}-\frac{\alpha}{4},1-\frac{\alpha}{4}\},\{\frac{1}{2},\frac{1}{2},1\},\frac{-\left(\mathrm{FR}^2\,z^2\right)}{256\,(1-z)^2})\,\sec(\frac{\alpha\,\pi}{4})}{128\,\frac{1}{256}^{\frac{\alpha}{4}}\,2^{\frac{\alpha}{2}}\left(\frac{1}{2}-\frac{\alpha}{4}\right)\left(1-\frac{\alpha}{4}\right)\left(-\frac{3}{2}+\frac{\alpha}{4}\right)FR^2\,\rho^2\,z^4\,\Gamma(-2+\frac{\alpha}{2})}+$$

$$\frac{\frac{1}{4}^{\frac{\alpha}{2}}\,\alpha\,\pi\left(\rho^2\,z^2\right)^{\frac{\alpha}{2}}\,\frac{\mathrm{FR}^2\,z^2}{(1-z)^2}^{\frac{3}{2}-\frac{\alpha}{4}}\,{}_pF_q(\{\frac{1}{2}-\frac{\alpha}{4},1-\frac{\alpha}{4}\},\{\frac{1}{2},\frac{1}{2},1\},\frac{-\left(\mathrm{FR}^2\,z^2\right)}{256\,(1-z)^2})\,\sec(\frac{\alpha\,\pi}{4})}{256\,\frac{1}{256}^{\frac{\alpha}{4}}\,2^{\frac{\alpha}{2}}\left(\frac{1}{2}-\frac{\alpha}{4}\right)\left(1-\frac{\alpha}{4}\right)\left(-\frac{3}{2}+\frac{\alpha}{4}\right)FR^2\,\rho^2\,z^4\,\Gamma(-2+\frac{\alpha}{2})}+$$

$$\frac{3\,\frac{1}{4}^{\frac{\alpha}{2}}\,\pi\left(\rho^2\,z^2\right)^{\frac{\alpha}{2}}\,\frac{\mathrm{FR}^2\,z^2}{(1-z)^2}^{\frac{3}{2}-\frac{\alpha}{4}}\,{}_pF_q(\{\frac{1}{2}-\frac{\alpha}{4},1-\frac{\alpha}{4}\},\{\frac{1}{2},\frac{1}{2},1\},\frac{-\left(\mathrm{FR}^2\,z^2\right)}{256\,(1-z)^2})\,\sec(\frac{\alpha\,\pi}{4})}{64\,\frac{1}{256}^{\frac{\alpha}{4}}\,2^{\frac{\alpha}{2}}\left(\frac{1}{2}-\frac{\alpha}{4}\right)\left(1-\frac{\alpha}{4}\right)\left(-\frac{3}{2}+\frac{\alpha}{4}\right)FR^2\,\rho^2\,z^3\,\Gamma(-2+\frac{\alpha}{2})}-$$

$$\frac{\frac{1}{4}^{\frac{\alpha}{2}}\,\alpha\,\pi\left(\rho^2\,z^2\right)^{\frac{\alpha}{2}}\,\frac{\mathrm{FR}^2\,z^2}{(1-z)^2}^{\frac{3}{2}-\frac{\alpha}{4}}\,{}_pF_q(\{\frac{1}{2}-\frac{\alpha}{4},1-\frac{\alpha}{4}\},\{\frac{1}{2},\frac{1}{2},1\},\frac{-\left(\mathrm{FR}^2\,z^2\right)}{256\,(1-z)^2})\,\sec(\frac{\alpha\,\pi}{4})}{128\,\frac{1}{256}^{\frac{\alpha}{4}}\,2^{\frac{\alpha}{2}}\left(\frac{1}{2}-\frac{\alpha}{4}\right)\left(1-\frac{\alpha}{4}\right)\left(-\frac{3}{2}+\frac{\alpha}{4}\right)FR^2\,\rho^2\,z^3\,\Gamma(-2+\frac{\alpha}{2})}-$$

$$\frac{3\,\frac{1}{4}^{\frac{\alpha}{2}}\,\pi\left(\rho^2\,z^2\right)^{\frac{\alpha}{2}}\,\frac{\mathrm{FR}^2\,z^2}{(1-z)^2}^{\frac{3}{2}-\frac{\alpha}{4}}\,{}_pF_q(\{\frac{1}{2}-\frac{\alpha}{4},1-\frac{\alpha}{4}\},\{\frac{1}{2},\frac{1}{2},1\},\frac{-\left(\mathrm{FR}^2\,z^2\right)}{256\,(1-z)^2})\,\sec(\frac{\alpha\,\pi}{4})}{128\,\frac{1}{256}^{\frac{\alpha}{4}}\,2^{\frac{\alpha}{2}}\left(\frac{1}{2}-\frac{\alpha}{4}\right)\left(1-\frac{\alpha}{4}\right)\left(-\frac{3}{2}+\frac{\alpha}{4}\right)FR^2\,\rho^2\,z^2\,\Gamma(-2+\frac{\alpha}{2})}+$$

$$\frac{\frac{1}{4}^{\frac{\alpha}{2}}\,\alpha\,\pi\left(\rho^2\,z^2\right)^{\frac{\alpha}{2}}\,\frac{\mathrm{FR}^2\,z^2}{(1-z)^2}^{\frac{3}{2}-\frac{\alpha}{4}}\,{}_pF_q(\{\frac{1}{2}-\frac{\alpha}{4},1-\frac{\alpha}{4}\},\{\frac{1}{2},\frac{1}{2},1\},\frac{-\left(\mathrm{FR}^2\,z^2\right)}{256\,(1-z)^2})\,\sec(\frac{\alpha\,\pi}{4})}{256\,\frac{1}{256}^{\frac{\alpha}{4}}\,2^{\frac{\alpha}{2}}\left(\frac{1}{2}-\frac{\alpha}{4}\right)\left(1-\frac{\alpha}{4}\right)\left(-\frac{3}{2}+\frac{\alpha}{4}\right)FR^2\,\rho^2\,z^2\,\Gamma(-2+\frac{\alpha}{2})},$$

where ${}_pF_q()$ is the generalized hypergeometric function. Integrating Eq. (A.2) symbolically over $\kappa$ gives

$$D_\phi(\rho) = 8\pi^2 k^2 a(\alpha)\int_0^1 \mathrm{d}z'\beta(z'L) \tag{A.4}$$

$$\frac{-\left(\sqrt{\pi}\,\frac{\rho^4\,(1-z)^2\,z^2}{\mathrm{FN}^2}^{-\frac{1}{2}+\frac{\alpha}{4}}\,\Gamma(\frac{3}{2}-\frac{\alpha}{4})\right)}{2\,(2-\alpha)\left(1-\frac{\alpha}{4}\right)(1-z)^2\,\Gamma(-1+\frac{\alpha}{4})}+\frac{\sqrt{\pi}\,z\,\frac{\rho^4\,(1-z)^2\,z^2}{\mathrm{FN}^2}^{-\frac{1}{2}+\frac{\alpha}{4}}\,\Gamma(\frac{3}{2}-\frac{\alpha}{4})}{(2-\alpha)\left(1-\frac{\alpha}{4}\right)(1-z)^2\,\Gamma(-1+\frac{\alpha}{4})}$$

$$-\frac{\sqrt{\pi}\,z^2\,\frac{\rho^4\,(1-z)^2\,z^2}{\mathrm{FN}^2}^{-\frac{1}{2}+\frac{\alpha}{4}}\,\Gamma(\frac{3}{2}-\frac{\alpha}{4})}{2\,(2-\alpha)\left(1-\frac{\alpha}{4}\right)(1-z)^2\,\Gamma(-1+\frac{\alpha}{4})}+\frac{\frac{1}{4}^{\frac{\alpha}{2}}\left(1-\frac{\alpha}{2}\right)\pi\left(\rho^2\,z^2\right)^{\frac{\alpha}{2}}\,\csc(\frac{\alpha\,\pi}{2})}{\left(-1+\frac{\alpha}{2}\right)\rho^2\,z^2\,\Gamma(\frac{\alpha}{2})^2}+$$

$$\frac{\sqrt{\pi}\,\frac{\rho^4\,(1-z)^2\,z^2}{\mathrm{FN}^2}^{-\frac{1}{2}+\frac{\alpha}{4}}\,\Gamma\left(\frac{3}{2}-\frac{\alpha}{4}\right)\,{}_{\mathrm{p}}F_{\mathrm{q}}\left(\left\{\frac{1}{2}-\frac{\alpha}{4},1-\frac{\alpha}{4}\right\},\left\{\frac{1}{2},\frac{1}{2},1\right\},\frac{-\left(\mathrm{FN}^2\,z^2\right)}{256\,(1-z)^2}\right)}{2\,(2-\alpha)\left(1-\frac{\alpha}{4}\right)(1-z)^2\,\Gamma\left(-1+\frac{\alpha}{4}\right)}$$

$$-\frac{\sqrt{\pi}\,z\,\frac{\rho^4\,(1-z)^2\,z^2}{\mathrm{FN}^2}^{-\frac{1}{2}+\frac{\alpha}{4}}\,\Gamma\left(\frac{3}{2}-\frac{\alpha}{4}\right)\,{}_{\mathrm{p}}F_{\mathrm{q}}\left(\left\{\frac{1}{2}-\frac{\alpha}{4},1-\frac{\alpha}{4}\right\},\left\{\frac{1}{2},\frac{1}{2},1\right\},\frac{-\left(\mathrm{FN}^2\,z^2\right)}{256\,(1-z)^2}\right)}{(2-\alpha)\left(1-\frac{\alpha}{4}\right)(1-z)^2\,\Gamma\left(-1+\frac{\alpha}{4}\right)}$$

$$+\frac{\sqrt{\pi}\,z^2\,\frac{\rho^4\,(1-z)^2\,z^2}{\mathrm{FN}^2}^{-\frac{1}{2}+\frac{\alpha}{4}}\,\Gamma\left(\frac{3}{2}-\frac{\alpha}{4}\right)\,{}_{\mathrm{p}}F_{\mathrm{q}}\left(\left\{\frac{1}{2}-\frac{\alpha}{4},1-\frac{\alpha}{4}\right\},\left\{\frac{1}{2},\frac{1}{2},1\right\},\frac{-\left(\mathrm{FN}^2\,z^2\right)}{256\,(1-z)^2}\right)}{2\,(2-\alpha)\left(1-\frac{\alpha}{4}\right)(1-z)^2\,\Gamma\left(-1+\frac{\alpha}{4}\right)}$$

$$+\frac{\sqrt{\pi}\,\frac{\rho^4\,(1-z)^2\,z^2}{\mathrm{FN}^2}^{-\frac{1}{2}+\frac{\alpha}{4}}\,\sqrt{\frac{\mathrm{FN}^2\,z^2}{(-1+z)^2}}\,\Gamma\left(1-\frac{\alpha}{4}\right)\,{}_{\mathrm{p}}F_{\mathrm{q}}\left(\left\{1-\frac{\alpha}{4},\frac{3}{2}-\frac{\alpha}{4}\right\},\left\{1,\frac{3}{2},\frac{3}{2}\right\},\frac{-\left(\mathrm{FN}^2\,z^2\right)}{256\,(1-z)^2}\right)}{32\,\Gamma\left(-\frac{1}{2}+\frac{\alpha}{4}\right)}.$$

## *Bibliography*


1. Beland, R. R. "Some aspects of propagation through weak isotropic non-Kolmogorov turbulence." Unpublished work.
2. Beland, R. R. "Propagation through atmospheric turbulence." *The Infrared and Electro-Optical Systems Handbook 2*, edited by F. G. Smith, chapter 2, 157–232, Infrared Information Analysis Center, Enviromental Research Institute of Michigan, 1993.
3. Bracewell, R. N. *The Fourier Transform and Its Applications* (2 Edition). McGraw Hill, 1978.
4. Buser, R. G. "Interferometric determination of the distance dependence of the phase structure function for near-ground horizontal propagation at 6328 angstroms," *J. Opt. Soc. Am.*, *61*(4):488–491 (April 1971).
5. Clifford, S. F. "The classical theory of wave propagation in a turbulent medium." *Laser Beam Propagation in the Atmosphere 25*. Topics in Applied Physics, edited by J. W. Strohbehn, chapter 2, 9–43, Springer-Verlag, 1978.
6. D. Dayton, et. al. "Atmospheric structure function measurements with a Shack-Hartmann wavefront sensor," *Optics Letters*, *17*(24):1737–1739 (December 1992).
7. F. Dalaudier, C. Sidi, M. Crochet and J. Vernin. "Direct evidence of sheets in the atmospheric temperature field," *J. Atmospheric Science* (1993).
8. Fried, D. L. "Optical resolution through a randomly inhomogeneous medium for very long and very short exposures," *J. Opt. Soc. Am.*, *56*:1372–1379 (1966).
9. Fried, D. L. "Optical heterodyne detection of an atmospherically distorted signal wave front," *Proc. IEEE*, *55*(1):57–67 (January 1967).
10. Goodman, J. W. *Statistical Optics*. New York: John Wiley & Sons, 1985.
11. Gurvich, A. S. "Model of three dimensional spectrum of local axisymmetric temperature inhomogeneities in stable stratified atmosphere.".
12. Heidbreder, G. R. "Image degradation with random wavefront tilt compensation," *IEEE Trans. Ant. Prop.*, *AP-15*:90–98 (1967).
13. Hill, R. J. and S. F. Clifford. "Modified spectrum of atmospheric temerature flucuations and its application to optical propagation," *J. Opt. Soc. Am.*, (68):892–899 (1978).
14. Hill, R. J. and D. O. Tarazano. *A Proposed Form for the Atmospheric Microtemperature Spatial Spectrum in the Input Range*. Technical Report, (RADC-TR-74-19) (ADA 776294/1GI) (Rome Air Development Center), 1974.

15. Kolmogorov, A. N. "The local structure of turbulence in incompressible viscous fluids for very large Reynolds' numbers." *Turbulence, Classic Papers on Statistical Theory* edited by S. K. Friedlander and L. Topper, 151–155, New York: Wiley-Interscience, 1961.

16. Lee, R. W. and J. C. Harp. "Weak scattering in random media, with applications to remote probing," *Proc. IEEE*, *57*:375–406 (1969).

17. Lutomirski, R. F. and R. G. Buser. "Mutual coherence function of a finite optical beam and application to coherent detection," *Appl. Opt.*, *12*:2153–2160 (1973).

18. Lutomirski, R. F. and H. T. Yura. "Propagation of a finite optical beam in an inhomogeneous medium," *Appl. Opt.*, *10*:1652–1658 (1971).

19. Marichev, O. I. *Handbook of Integral Transforms of Higher Transcendental Functions*. Ellis Horwood Limited, 1983.

20. Noll, Robert J. "Zernike polynomials and atmospheric turbulence," *J. Opt. Soc. Am.*, *66*:207–211 (1976).

21. Roddier, F. "The effects of atmospheric turbulence in optical astronomy." *Progress in Optics XIX*, edited by E. Wolf, New York: North–Holland, 1981.

22. Sasiela, R. *Draft: Electromagnetic Wave Propagation in Turbulence: A Mellin Transform Approach*. Technical Report, MIT/Lincoln Laboratory, March 1992.

23. Sasiela, R. J. *A Unified Approach to Electromagnetic Wave Propagation in Turbulence and the Evaluation of Multiparameter Integrals*. Technical Report TR 807, Lincoln Laboratory, Massachusetts Institute of Technology, June 1988.

24. Sasiela, R. J. and J. D. Shelton. "Mellin transform methods applied to integral evaluation: Taylor series and asymptotic approximations," *Journal of Mathematical Physics*, *34*(6):2572–2619 (June 1993).

25. Tatarski, V. I. *Wave Propagation in a Turbulent Medium*. New York: Dover Publications, 1967.

26. Tatarski, V. I. *The Effects of the Turbulent Atmosphere on Wave Propagation*. Technical Report, U. S. Dept of Commerce, National Technical Information Service, 1971.

27. von Karman, T. "Progress in the statistical theory of turbulence." *Turbulence, Classic Papers on Statistical Theory* edited by S. K. Friedlander and L. Topper, 162–174, Wiley-Interscience, 1961.

28. Wissler, J. (April 1994). personal communication.

29. Wolfram, S. *Mathematica: A System for Doing Mathematics by Computer* (2 Edition). Addison-Wesley, 1991.

30. Yura, H. T. "Mutual coherence function of a finite cross section optical beam propagating in a turbulent medium," *Appl. Opt.*, *11*:1399–1406 (1972).

## *Vita*

Capt Bruce Stribling received a Bachelor of Science degree in Electrical Engineering from the University of Nevada-Reno in December, 1985. Upon graduation he was commissioned as a second lieutenant in the United States Air Force, where he was assigned to the Ballistic Missile Office as a Guidance and Control System Project Officer for the Peacekeeper, Peacekeeper Rail Garrison, and Minuteman III intercontinental ballistic missile (ICBM) programs. In September 1991, Capt Stribling was transferred to Wright Laboratory to conduct research on fiber optic flight control systems. He is currently assigned to the Air Force Institute of Technology where he is conducting thesis research on the propagation of light through non-Kolmogorov atmospheric turbulence. Upon graduation from AFIT he will be assigned to Phillips Laboratory's Air Force Maui Optical Station (AMOS) where he will be conducting research on advanced imaging techniques.

Permanent address: 3011 Brandywine Ave.
Anchorage, AK 99502

# REPORT DOCUMENTATION PAGE

Form Approved
OMB No. 0704-0188



| 1. AGENCY USE ONLY (Leave blank) | 2. REPORT DATE | 3. REPORT TYPE AND DATES COVERED |
|---|---|---|
| | 13 Dec 1994 | Master's Thesis |

**4. TITLE AND SUBTITLE**

Laser Beam Propagation in Non-Kolmogorov Atmospheric Turbulence

**5. FUNDING NUMBERS**

**6. AUTHOR(S)**

Bruce E. Stribling, Capt, USAF

**7. PERFORMING ORGANIZATION NAME(S) AND ADDRESS(ES)**

Air Force Institute of Technology, WPAFB OH 45433-6583

**8. PERFORMING ORGANIZATION REPORT NUMBER**

AFIT/GEO/ENG/94D-04

**9. SPONSORING/MONITORING AGENCY NAME(S) AND ADDRESS(ES)**

Capt Brian Scruggs
PL/LIAF
3550 Aberdeen S.W.
KAFB, NM 87117-5776

**10. SPONSORING/MONITORING AGENCY REPORT NUMBER**

**11. SUPPLEMENTARY NOTES**

**12a. DISTRIBUTION/AVAILABILITY STATEMENT**

Approved for Public Release; Distribution Unlimited

**12b. DISTRIBUTION CODE**

**13. ABSTRACT** *(Maximum 200 words)*

Several observations of atmospheric turbulence statistics have been reported which do not obey Kolmogorov's power spectral density model. These observations have prompted the study of optical propagation through turbulence described by non-classical power spectra. This thesis presents an analysis of optical propagation through turbulence which causes index of refraction fluctuations to have spatial power spectra that obey arbitrary power laws. The spherical and plane wave structure functions are derived using Mellin transform techniques and are applied to the field mutual coherence function (MCF) using the extended Huygens-Fresnel principle. The MCF is used to compute the Strehl ratio of a focused, constant amplitude beam propagating in non-Kolmogorov turbulence as the power law for the spectrum of the index of refraction fluctuations is varied from -3 to -4. The relative contributions of the log amplitude and phase structure functions to the wave structure function are computed. If inner and outer scale effects are neglected, no turbulence exists when the power law equals -3. At power laws close to -3, the magnitude of the log amplitude and phase perturbations are determined by the system Fresnel ratio. At power laws approaching -4, phase effects dominate in the form of random tilts.

**14. SUBJECT TERMS**

Kolmogorov, Mellin Transforms, Laser Beam Propagation, Turbulence, Structure Function, Huygens-Fresnel, Strehl Ratio

**15. NUMBER OF PAGES**

90

**16. PRICE CODE**

| 17. SECURITY CLASSIFICATION OF REPORT | 18. SECURITY CLASSIFICATION OF THIS PAGE | 19. SECURITY CLASSIFICATION OF ABSTRACT | 20. LIMITATION OF ABSTRACT |
|---|---|---|---|
| UNCLASSIFIED | UNCLASSIFIED | UNCLASSIFIED | UL |